FIRST PRINCIPLES INVESTIGATION OF ELECTRONIC AND MAGNETIC PROPERTIES OF HALF-METALLIC HEUSLER ALLOYS

2011
M.Sc. Thesis
Physics

Ulvi KANBUR

FIRST PRINCIPLES INVESTIGATION OF ELECTRONIC AND MAGNETIC PROPERTIES OF HALF-METALLIC HEUSLER ALLOYS

A THESIS SUBMITTED TO
THE GRADUATE SCHOOL OF NATURAL AND APPLIED SCIENCES
OF
KARABÜK UNIVERSITY

BY

Ulvi KANBUR

IN PARTIAL FULFILLMENT OF THE REQUIREMENTS
FOR
THE DEGREE OF MASTER OF SCIENCE
IN
DIVISION OF PHYSICS

July 2011

I certify that in my opinion the thesis submitted by Ulvi KANBUR titled "FIRST PRINCIPLES INVESTIGATION OF ELECTRONIC AND MAGNETIC PROPERTIES OF HALF-METALLIC HEUSLER ALLOYS" is fully adequate in scope and in quality as a thesis for the degree of Master of Science.

Assist. Prof. Dr. Gökhan GÖKOĞLU
Thesis Advisor, the Division of Physics

This thesis is accepted by the examining committee with a unanimous vote in the Division of Physics as a master thesis. June 22, 2011

Examining Committee Members (Institutions)	Signature
Chairman : Assist. Prof. Dr. Mustafa ANUTGAN (KBÜ)	
Member : Assist. Prof. Dr. Gökhan GÖKOĞLU (KBÜ)	
Member : Assist. Prof. Dr. Hasan YILDIRIM (KBÜ)	

....., 2011

The degree of Master of Science by the thesis submitted is approved by the Administrative Board of the Graduate School of Natural and Applied Sciences, Karabük University.

Assoc. Prof. Dr. Nizamettin KAHRAMAN
Head of Graduate School of Natural and Applied Sciences

“I declare that all the information within this thesis has been gathered and presented in accordance with academic regulations and ethical principles and I have, according to the requirements of these regulations and principles, cited all those which do not originate in this work as well.”

Ulvi KANBUR

ABSTRACT

M.Sc. Thesis

FIRST PRINCIPLES INVESTIGATION OF ELECTRONIC AND MAGNETIC PROPERTIES OF HALF-METALLIC HEUSLER ALLOYS

Ulvi KANBUR

Karabük University
Graduate School of Natural and Applied Science
the Division of Physics

Thesis Advisor
Assist. Prof. Dr. Gökhan GÖKOĞLU
July 2011, 48 pages

In this study, we present the electronic, magnetic, and structural properties of two novel half-metallic full-Heusler compounds, $\mathrm{Co_2CrAs}$ and $\mathrm{Co_2CrSb}$, in cubic $\mathrm{L2_1}$ geometry. The calculations are based on the density functional theory within plane-wave pseudopotential method and spin-polarized generalized gradient approximation of the exchange-correlation functional. The electronic band structures and density of states of the systems indicate half-metallic behavior with vanishing electronic density of states of minority spins at Fermi level, which yields perfect spin polarization. The calculated magnetic moments of both systems in $\mathrm{L2_1}$ structure are $5.00\mu_B$, which are largely localized on the chromium site. The energy gaps in minority spin states are restricted by the $\mathrm{3d}$-states of cobalt atoms on two different sublattices. The formation enthalpies for both structures are negative indicating stability of these systems against decomposition into stable solid compounds.

Key Words : Ab initio calculation, half-metal, electronic structure, heusler alloys

Science Code : 202.1.166

ÖZET

Yüksek Lisans Tezi

YARI-METALİK HEUSLER ALAŞIMLARININ ELEKTRONİK VE MANYETİK ÖZELLİKLERİNİN İLK PRENSİPLERDEN İNCELENMESİ

Ulvi KANBUR

Karabük Üniversitesi
Fen Bilimleri Enstitüsü
Fizik Ana Bilim Dalı

Tez Danışmanı
Yrd. Doç. Dr. Gökhan GÖKOĞLU
Temmuz 2011, 48 sayfa

Bu çalışmada, kübik $\mathrm{L2_1}$ geometrisine sahip iki yeni yarı-metalik tam-Heusler bileşikleri olan $\mathrm{Co_2CrAs}$ ve $\mathrm{Co_2CrSb}$ için elektronik, menyetik ve yapısal özellikler verilmiştir. Hesaplamalar, düzlem dalga sözde-potansiyel metodu ve değiş tokuş korelasyon fonksiyonelleri için spin-polarize genelleştirilmiş gradyan yaklaşımı ışığında yoğunluk fonksiyoneli teorisine dayanmaktadır. Sistemlerin elektronik bant yapıları ve durum yoğunlukları, Fermi düzeyinde aşağı spin elektronik durum yoğunlukarının sıfırlanması ile tam bir spin polarizasyonu oluşturarak yarı-metalik karakter göstermektedir. Her iki sistemin $\mathrm{L2_1}$ yapısında hesaplanan manyetik momentleri $5.00\mu_B$ değerindedir ve büyük ölçüde krom atomu kaynaklıdır. Aşağı spin durumlarında enerji boşlukları, iki farklı alt örgüdeki kobalt atomlarının $\mathrm{3d}$ durumları tarafından sınırlandırılmıştır. Sistemlerin oluşma entalpileri negatif değere sahiptir ve kendini oluşturan elementlerin katı bileşikerine bozulmaya karşı kararlılığını gösterir.

Anahtar Sözcükler : İlk prensip hesabı,yarı-metal, elektronik yapı, Heusler alaşımları
Bilim Kodu : 202.1.166

ACKNOWLEDGMENTS

Foremost, I would like to express my sincere gratitude to my advisor Assist. Prof. Dr. Gökhan GÖKOĞLU (Karabük University) for the continuous support of my M.Sc. study and research.

My sincere thanks also goes to Res. Assist. Savaş AĞDUK (Karabük University) for the computational tricks on high performance computing.

I thank to The Scientific & Technological Research Council of Turkey through TR-Grid e-Infrastructure for carrying out the part of the calculations at Turkish Academic Network and Information Center.

CONTENTS

Page

Page

LIST OF FIGURES

Page

LIST OF TABLES

Page

SYMBOLS AND ABBREVIATIONS INDEX

ABBREVIATIONS

SCF	: Self-Consistent Field
TF	: Thomas-Fermi
HK	: Hohenberg-Kohn
XC	: Exchange-Correlation
L(S)DA	: Local (Spin) Density Approximation
GEA	: Gradient Expansion Approximation
GGA	: Generalized Gradient Approximation
GMR	: Giant Magnetoresistance
DOS	: Density of States

PART 1

INTRODUCTION

One of the basic problems in theoretical physics is the description of the structure and dynamics of many-electron systems comprising single atoms, the most elementary building blocks of ordinary matter, all kinds of molecules, etc [1]. For polyatomic molecules, the presence of several nuclei makes quantum-mechanical calculations harder than for diatomic molecules. Moreover, the electronic wavefunction of a diatomic molecule is a function of only one parameter—the inter nuclear distance [2]. In contrast, the electronic wave function of a polyatomic molecule depends on several parameters—the bond distances, bond angles, and dihedral angles of rotation about single bonds (these angles define the molecular conformation). A full theoretical treatment of a polyatomic molecule involves calculation of the electronic wavefunction for a range of each of these parameters [2].

The calculation of geometries and energies of molecules can be investigated by three techniques: molecular mechanics, *ab initio* methods, and semiempirical methods. Both ab initio and semiempirical methods are based on quantum mechanics with Schrödinger equation and calculate a molecular wavefunction and molecular orbital energies [3].

The first calculations handled on many-body systems by D. R. Hartree and E. Hylleraas were for atoms. Hartree's method today is still in use for numerical calculations known as self-consistent field (SCF) method, in which each electron moves in a central potential due to the nucleus and other electrons. In 1930, Fock published the first calculations by using a antisymmetrized determinant wavefunctions, known as the Hartree-Fock method. Hylleraas provided accurate solutions for the ground state of two-electron systems as early as 1930 [4].

However, a wavefunction is not a measurable quantity of an atom or molecule, i.e. not an observable. Density Functional Theory, DFT, is not based on the wavefunction, but rather on the electron probability density function or electron density function. Unlike the wavefunctions, charge density is measurable. The main advantage of electron density is that it is a function of position only comprising three coordinates [3].

1.1. HISTORY OF DFT

The modern progress of DFT uses a philosophy which in a manner of speaking starts from exploiting a one-to-one correspondence between particle densities $\rho(\boldsymbol{r})$ and many-body wavefunctions $\psi(x_1, x_2, \ldots, x_N)$ of ground states. One tries to find a functional expression of the ground state energy E through the ground state density $\rho(\boldsymbol{r})$ instead of the two-particle density matrix, and then to base a variational principle for the density on that functional relation.

Thomas-Fermi theory is the earliest and most naive version of such theories, which uses the electron density rather than the wavefunction for obtaining information about atomic and molecular systems. E. Fermi and P. A. M. Dirac independently made calculations on an ideal electron gas delivering that atomic and molecular properties can be investigated by use of electron density [5]. In an independent work by Fermi and Thomas, atoms were thought with a positive potential located in a uniform (homogeneous) electron gas. Thomas-Fermi model has given good results for atoms, but failed for molecules: it has predicted all molecules to be unstable toward dissociation into their atoms [3].

The $\mathrm{X}\alpha$ (X =exchange, α is a parameter in the $\mathrm{X}\alpha$ equation) method [6] by Slater, a more accurate version of Thomas-Fermi model introduced in 1951, was the first useful DFT model. Slater regarded it as a simplification of the Hartree-Fock approach. The $\mathrm{X}\alpha$ method was developed mainly for atoms and solids and has also been used for molecules, and has been replaced by more accurate Kohn-Sham type DFT method [3].

1.2. THE THOMAS-FERMI MODEL

To investigate the atomic and molecular properties of systems, the electron density was firstly used by Thomas and Fermi with a simple quantum statistical model which takes into account only the kinetic energy term of the many body problem while treating others in a classical way. In their model, Thomas and Fermi arrive at the following, very simple expression for the kinetic energy based on the uniform electron gas, a fictitious model system of constant electron density [5],

$$T_{TF}[\rho(\boldsymbol{r})] = \frac{3}{10}(3\pi^2)^{2/3}\int \rho(\boldsymbol{r})^{5/3}\,\mathrm{d}\boldsymbol{r} \tag{1.1}$$

If this is combined with the classical expression for the nuclear-electron attractive potential and the electron-electron repulsive potential we have the famous Thomas-Fermi expression for the energy of an atom,

$$E_{TF}[\rho(\boldsymbol{r})] = \frac{3}{10}(3\pi)^2\int \rho(\boldsymbol{r})^{5/3}\,\mathrm{d}\boldsymbol{r} - Z\int \frac{\rho(\boldsymbol{r})}{r}\,\mathrm{d}\boldsymbol{r} + \frac{1}{2}\iint \frac{\rho(\boldsymbol{r_1})\rho(\boldsymbol{r_1})}{|\boldsymbol{r}_1-\boldsymbol{r}_2|}\,\mathrm{d}\boldsymbol{r}_1\,\mathrm{d}\boldsymbol{r}_2. \tag{1.2}$$

As mentioned, Thomas-Fermi approach is only a coarse approximation to the true kinetic energy and, exchange and correlation effects are completely neglected. But the importance of this equation arises from the fact that the energy is given completely in terms of the electron density $\rho(\boldsymbol{r})$.

Thus we have the first example of a density functional for the energy. In other words, Eq. 1.2 is a prescription for how to map a density $\rho(\boldsymbol{r})$ onto an energy E without any additional information required. In particular no recourse to the wavefunction is taken.

1.3. THE HOHENBERG-KOHN THEOREMS

The histories of the Thomas-Fermi and Hohenberg-Kohn theories present instructive examples of the way knowledge is gathered in many-body physics [7]. The starting point of any discussion of DFT is the Hohenberg-Kohn (HK) theorem. The approach of Hohenberg and Kohn is to formulate DFT as an exact theory of many-body systems [4].

A paper published in 1964 by Hohenberg and Kohn [8] vitalized DFT after the studies of Thomas, Fermi, and Dirac in early years. Theorems proven in that research were the pillars of modern DFT. This section discusses these theorems and their consequences. We will focus on how a physically meaningful wavefunction can be uniquely related to a density, i.e. to electron density.

1.3.1. The First Hohenberg-Kohn Theorem

Quoting directly from the Hohenberg-Kohn paper [8], the first theorem states that '*the external potential $V_{ext}(\boldsymbol{r})$ is (to within a constant) a unique functional of $\rho(\boldsymbol{r})$; since, in turn $V_{ext}(\boldsymbol{r})$ fixes $\hat{\boldsymbol{H}}$ we see that the full many particle ground state is a unique functional of $\rho(\boldsymbol{r})$*' [5]. In other words, given $\rho(\boldsymbol{r})$ we can in principle calculate any ground state property, e.g. the energy, E_0.

The theorem is merely an existence theorem: it says that a functional F exists, but does not tell us how to find it; this omission is the main problem with DFT [3]. For the proof [4, 5] we consider two external potentials V_{ext} and V'_{ext} (differ by more than a constant) which give the same electron density $\rho(\boldsymbol{r})$ (for non-degenerate case). The external potentials lead to two different hamiltonians $\hat{H}$ and $\hat{H}'$ which have different ground state wavefunctions, Ψ and Ψ' with the same ground state density $\rho_0(\boldsymbol{r})$. Since ψ' is not the ground state of $\hat{H}$, it follows that,

$$E_0 < \langle \Psi' | \hat{H} | \Psi' \rangle = \langle \Psi' | \hat{H}' | \Psi' \rangle + \langle \Psi' | \hat{H} - \hat{H}' | \Psi' \rangle \tag{1.3}$$

which yields

$$E_0 < E'_0 + \langle \Psi' | \hat{V}_{ext} - \hat{V}'_{ext} | \Psi' \rangle . \tag{1.4}$$

By the same trick we have

$$E'_0 < E_0 - \langle \Psi' | \hat{V}_{ext} - \hat{V}'_{ext} | \Psi' \rangle . \tag{1.5}$$

After adding equations (1.4) and (1.5) we get the desired result $E + E' < E' + E$ which means that there cannot be two different external potentials that yield the same non-degenerate ground state electron density.

1.3.2. The Second Hohenbergh-Kohn Theorem

It has been emphasized that the ground state electron density determines all property of the system in interest. But how can we be sure that the above density is the true ground state density that we are looking for? Second theorem says that a density functional gives the ground state energy of the system if and only if the input density is the true ground state density. For the proof [5], we again refer to the variational principle which can be expressed as

$$E_0 \leq E[\rho'] = T[\rho'] + E_{Ne}[\rho'] + E_{ee}[\rho']. \tag{1.6}$$

where T, E_{Ne} and E_{ee} are kinetic energy, nucleus-electron and electron-electron interactions of particles. Any trial density ρ' has a corresponding wavefunction Ψ' which can be used as the trial wavefunction for the true Hamiltonian to give the desired result as following,

$$\langle \Psi' | \hat{H} | \Psi' \rangle = T[\rho'] + E_{ee}[\rho'] + \int \rho' V_{ext} d\boldsymbol{r} = E[\rho'] \geq E_0[\rho_0] = \langle \Psi | \hat{H} | \Psi \rangle \tag{1.7}$$

in which the integral term gives E_{Ne}.

1.4. THE KOHN-SHAM APPROACH

Now we will apply the HK theorems to our problem. The second major contribution to the DFT was made by Kohn and Sham in 1965 in which the kinetic energy was determined in an ingenious way [9]. Kohn and Sham proposed introducing orbitals into the problem in such a way that the kinetic energy can be computed simply to good accuracy, leaving a small residual correction that is handled separately [10]. According to HK theorems, our fundamental quantity was electron density. We can write ground

state energy of an atomic or molecular system as

$$E_0 = \min\left(F[\rho] + \int \rho(\boldsymbol{r}) V_{Ne} d\boldsymbol{r}\right) \tag{1.8}$$

where V_{Ne} is the potential due to the nuclei-electron interaction, and

$$F[\rho(\boldsymbol{r})] = T[\rho(\boldsymbol{r})] + E_{ee}[\rho(\boldsymbol{r})] \tag{1.9}$$

is the HK functional which is a universally valid term i.e. its form is independent of N, R_A and Z_A which denotes number of electrons, spatial coordinates of nuclei and nuclear charge of indexed atom, respectively. We can split E_{ee} term by extracting Coulomb part

$$E_{ee}[\rho] = \frac{1}{2}\int\int \frac{\rho(\boldsymbol{r_1})\rho(\boldsymbol{r_2})}{r_{12}} d\boldsymbol{r_1} d\boldsymbol{r_2} + E_{ncl}[\rho] = J[\rho] + E_{ncl}[\rho] \tag{1.10}$$

in which $E_{ncl}[\rho]$ is the *non-classical* contribution to the electron-electron interaction. Thus we have the final but not ultimate form of HK functional as

$$F[\rho(\boldsymbol{r})] = T[\rho] + J[\rho] + E_{ncl}[\rho]. \tag{1.11}$$

Through these terms only $J[\rho]$ is known while other two remain a mystery. Kohn and Sham treated the kinetic energy term in a different way for better accuracy. They separated the functional $F[\rho]$ by extracting the exact non-interacting part of kinetic energy term while combining the residue with the remaining unknown term. Ultimately we have a functional with two exact terms and one combined unknown term as

$$F[\rho(\boldsymbol{r})] = T_S[\rho] + J[\rho] + E_{XC}[\rho]. \tag{1.12}$$

The first term T_S stands for the non-interaction contribution to kinetic energy and the last term is the so-called *exchange-correlation energy* which is defined as

$$E_{XC}[\rho] = T_C[\rho] + E_{ncl}[\rho] \tag{1.13}$$

in which $T_C[\rho]$ is the residual part of the kinetic energy. As can be understood easily the term E_{XC} contains everything unknown. What can we say about the non-interacting kinetic energy term $T_S[\rho]$? We know mathematically that the solution to a system which consists of N non-interacting particles ,is exactly an N dimensional Slater determinant. We immediately write the term explicitly as follows,

$$T_S = -\frac{1}{2}\sum_{i}^{N} \langle\psi_i| \nabla^2 |\psi_i\rangle \tag{1.14}$$

It is clear from the result that ψ_is are spin orbitals. If we write explicitly all terms of the electronic Hamiltonian except for one (which is of course the unknown) we get

$$\begin{aligned} E[\rho(\boldsymbol{r})] &= T_S[\rho] + J[\rho] + E_{XC}[\rho] + E_{Ne}[\rho] && (1.15)\\ &= -\frac{1}{2}\sum_{i}^{N} \langle\psi_i| \nabla^2 |\psi_i\rangle + \frac{1}{2}\sum_{i,j}^{N} \int |\psi_i(\boldsymbol{r_1})|^2 \frac{1}{r_{12}} |\psi_j(\boldsymbol{r_2})|^2 d\boldsymbol{r_1} d\boldsymbol{r_2} \\ &\quad + E_{XC}[\rho] - \sum_{i}^{N} \int \sum_{A}^{M} \frac{Z_A}{r_{1A}} |\psi_i(\boldsymbol{r_1})|^2 d\boldsymbol{r_1}. && (1.16) \end{aligned}$$

By using the variational principle with constraint $\langle\psi_i|\psi_j\rangle = \delta_{ij}$ the above expression results following Kohn-Sham (KS) one electron equations [10]

$$\left(-\frac{1}{2}\nabla^2 + \int \frac{\rho(\boldsymbol{r_2})}{r_{12}} d\boldsymbol{r_2} + V_{XC}(\boldsymbol{r_1}) - \sum_{A}^{M} \frac{Z_A}{r_{1A}} \right) \psi_i = \epsilon_i \psi_i \tag{1.17}$$

which have to be solved iteratively. A schematic diagram is shown in Figure 1.1. The only approximations in these equations arise from the functional for the exchange-correlation energy E_{XC} and the corresponding potential V_{XC}.

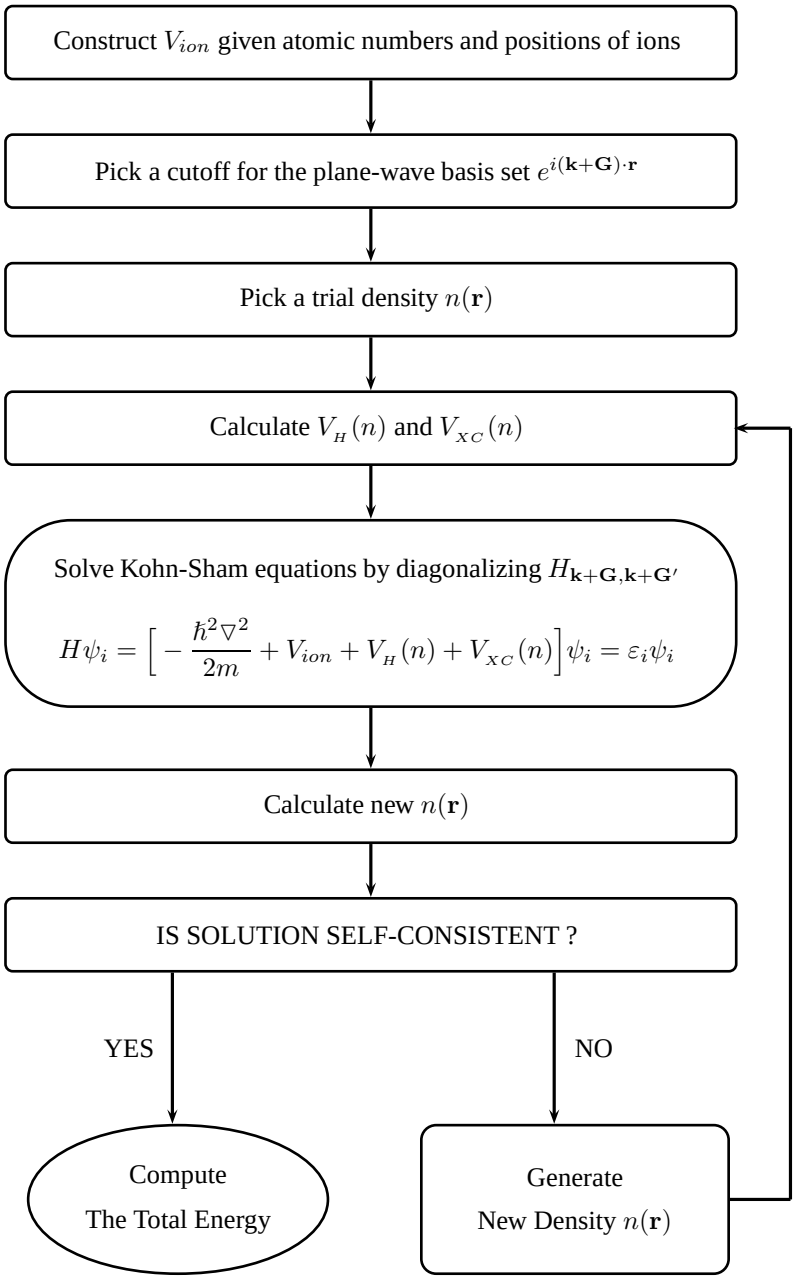

Figure 1.1. Schematic representation of the self-consistent loop for solution of KS equations.

1.5. EXCHANGE-CORRELATION ENERGY FUNCTIONAL

We introduced the KS formalism which allows an exact treatment of most of the contributions to the electronic energy of an atomic or molecular system, including the major fraction of the kinetic energy. In this section, we briefly introduce the approximations used for the xc-energy functional. The presentation focuses on the

derivation of the most important functionals, and their results, the local density and generalized gradient approximations. The quality of the density functional approach hinges solely on the accuracy of the chosen approximation to E_{XC} [5].

1.5.1. Local (Spin) Density Approximation: L(S)DA

Kohn and Sham pointed out that solids can often be considered as close to the limit of the uniform electron gas [4]. The simple concept of the local density approximation is based on the *uniform electron gas*, which represents the bedrock of almost all current functionals. This is a system in which electrons move on a positive background charge distribution such that the total ensemble is electrically neutral. We continue with a discussion of the problems due to the self-interaction of the charge density and to the behavior of the corresponding exchange-correlation potentials in the long range asymptotic region [5].

The number of electrons N as well as the volume V of the gas are considered to approach infinity, while the electron density, N/V remains finite, and attains a constant value everywhere. The uniform electron gas is a fairly good physical model for simple metals. We can write E_{XC} in the following form [4],

$$E_{XC}^{L(S)DA}[\rho^{\uparrow},\rho^{\downarrow}] = \int \rho(\boldsymbol{r})\epsilon_{XC}(\rho^{\uparrow}(\boldsymbol{r}),\rho^{\downarrow}(\boldsymbol{r}))\,\mathrm{d}\boldsymbol{r}\,. \tag{1.18}$$

Here, $\epsilon_{XC}(\rho^{\uparrow}(\boldsymbol{r}),\rho^{\downarrow}(\boldsymbol{r}))$ is the exchange-correlation energy per particle of a uniform electron gas of density $\rho(\boldsymbol{r})$. Writing E_{XC} in this way defines the *local spin density approximation*, L(S)DA for short. The quantity $\epsilon_{XC}(\rho^{\uparrow}(\boldsymbol{r}),\rho^{\downarrow}(\boldsymbol{r}))$ can be further split into exchange and correlation contributions,

$$\epsilon_{XC}(\rho^{\uparrow}(\boldsymbol{r}),\rho^{\downarrow}(\boldsymbol{r})) = \epsilon_X(\rho^{\uparrow}(\boldsymbol{r}),\rho^{\downarrow}(\boldsymbol{r})) + \epsilon_C(\rho^{\uparrow}(\boldsymbol{r}),\rho^{\downarrow}(\boldsymbol{r}))\,. \tag{1.19}$$

The first term on the right hand side of the last equation, ϵ_X, represents the exchange energy of an electron in a uniform electron gas of a particular density. This term has the form Slater found in his approximation of Hartree-Fock exchange and was originally

derived by Bloch and Dirac in the late 1920s [5]:

$$\epsilon_X = -\frac{3}{4}\left(\frac{3\rho(\boldsymbol{r})}{\pi}\right)^{1/3} . \tag{1.20}$$

No such explicit expression is known for the correlation part, ϵ_C. Many analytical expressions of ϵ_C have been presented based on sophisticated interpolation schemes. The most widely used one was developed by Vosko, Wilk, and Nusair [11], and the most recent and probably the most accurate one has been given by Perdew and Wang [12].

If we restrict the L(S)DA to the unpolarized case, we arrive at the *local density approximation* (LDA). We now write

$$E_{XC}^{LDA}[\rho] = \int \rho(\boldsymbol{r})\, \epsilon_{XC}(\rho(\boldsymbol{r}))\, \mathrm{d}\boldsymbol{r} . \tag{1.21}$$

Just as for the simple, spin compensated situation where $\rho^{\uparrow}(\boldsymbol{r}) = \rho^{\downarrow}(\boldsymbol{r}) = (1/2)\rho(\boldsymbol{r})$ there are related expressions for the exchange and correlation energies per particle of the uniform electron gas characterized by $\rho^{\uparrow}(\boldsymbol{r}) \neq \rho^{\downarrow}(\boldsymbol{r})$ the so-called spin polarized case.

1.5.2. The Generalized Gradient Approximation: GGA

For many years the LDA has been the only approximation available for E_{XC}. This situation changed when the first successful extension to the purely local approximation as developed. The use of not only the information about the density $\rho(\boldsymbol{r})$ at a particular point $\boldsymbol{r}$, but the *gradient* of the charge density, $\boldsymbol{\nabla}\rho(\boldsymbol{r})$, has also been suggested in order to account for the non-homogeneity of the true electron density. In other words, we interpret the local density approximation as the first term of a Taylor expansion of the uniform density and expect to obtain better approximations of the exchange-correlation functional by extending the series with the next lowest term [5]. Thus we arrive at the functional

$$E_{XC}^{GEA}[\rho^{\uparrow},\rho^{\downarrow}] = \int \rho\, \epsilon_{XC}(\rho^{\uparrow},\rho^{\downarrow})\,\mathrm{d}\boldsymbol{r} + \sum_{\sigma,\sigma'}\int C_{XC}^{\sigma,\sigma'}(\rho^{\uparrow},\rho^{\downarrow})\frac{\boldsymbol{\nabla}\rho_{\sigma}}{\rho_{\sigma}^{2/3}}\frac{\boldsymbol{\nabla}\rho_{\sigma'}}{\rho_{\sigma'}^{2/3}}\,\mathrm{d}\boldsymbol{r} + \cdots \tag{1.22}$$

called *gradient expansion approximation* (GEA) and that can be applied to a model system where the density is not uniform but varies slowly. Unfortunately the GEA does not lead to desired improvement even frequently worse than the simple LDA when applied to real molecular problems. The reason for this failure is that the exchange-correlation hole associated with a functional has lost many of the properties which made the LDA hole physically meaningful. Thus, the dependence between the depth of the on-top hole and its extension is lost and the holes as well as the corresponding exchange-correlation energies will be much more erratic [5].

This problem was solved by setting parts to zero in the GEA exchange holes violating the requirement of being negative everywhere and truncating the exchange and correlation holes such that $h_X(\boldsymbol{r}_1;\boldsymbol{r}_2)$ and $h_C(\boldsymbol{r}_1;\boldsymbol{r}_2)$ which contain one and zero electron charges, respectively. Functionals that include the gradients of the charge density and where the hole constraints have been restored in the above manner are collectively known as *generalized gradient approximations* (GGA). These functionals have the form [5]

$$E_{XC}^{GGA}[\rho^{\uparrow},\rho^{\downarrow}] = \int f(\rho^{\uparrow},\rho^{\downarrow},\boldsymbol{\nabla}\rho^{\uparrow},\boldsymbol{\nabla}\rho^{\downarrow})\,\mathrm{d}\boldsymbol{r} = E_X^{GGA} + E_C^{GGA} \tag{1.23}$$

in which the exchange part is rewritten as

$$E_X^{GGA} = E_X^{LDA} - \sum_{\sigma}\int F(s_{\sigma})\rho_{\sigma}^{4/3}(\boldsymbol{r})\,\mathrm{d}\boldsymbol{r}. \tag{1.24}$$

where the argument of F is the *reduced density gradient* for spin σ and given by

$$s_{\sigma}(\boldsymbol{r}) = \frac{|\boldsymbol{\nabla}\rho_{\sigma}(\boldsymbol{r})|}{\rho_{\sigma}^{4/3}(\boldsymbol{r})} \tag{1.25}$$

and must be understood as a local inhomogeneity parameter.

For the function F two main classes of realizations have been put forward. The first includes functionals with empirical parameters and the second includes functionals that use a rational functional of the reduced density gradient for F and have fewer empirical parameters. The prominent representations are the early functionals by Becke, 1986 (B86) [13] and Perdew, 1986 (P) [14], the functional by Lacks and Gordon, 1993 (LG) [15] or the recent implementation of Perdew, Burke, and Ernzerhof, 1996 (PBE) [16]. As an example, we explicitly write down F of Perdew's 1986 exchange functional, which, just as for the more recent PBE functionals, is free of semiempirical parameters:

$$F^{P86} = \left(1+1.296\left(\frac{s_\sigma}{(24\pi^2)^{1/3}}\right)^2+14\left(\frac{s_\sigma}{(24\pi^2)^{1/3}}\right)^4+0.2\left(\frac{s_\sigma}{(24\pi^2)^{1/3}}\right)^6\right)^{1/15} \quad (1.26)$$

For the functional E_C^{GGA}, more complicated analytical forms exist and cannot be understood by simple physically motivated reasonings. As examples, the most widely used choice is the correlation counterpart of the 1986 Perdew exchange functional. A few years later Perdew and Wang, 1991, refined their correlation functional, leading to the parameter free PW91. Another, nowadays even more popular one, is due to Lee, Yang, and Parr, 1988 (LYP) [17] which contains one empirical parameter. It should be noted that all correlation functions are based on systems that *only* include short range correlation effects.

1.6. PLANE-WAVES AND PSEUDOPOTENTIALS

The fundamental idea of a pseudopotential is the replacement of a problem with a simpler one. The primary application in electronic structure is to replace the strong Coulomb potential of the nucleus and effects of the tightly bounded core electrons by an effective ionic potential acting on the valence electrons [4] as shown in Figure 1.2.

The elements with atomic number 19 or more have a significant slowing effect on ab-initio calculations because of the many two-electron repulsion integrals. The usual way of overcoming this problem is adding to the Fock operator a one-electron operator that takes into account the effect of the core electrons in a collective way on the valence

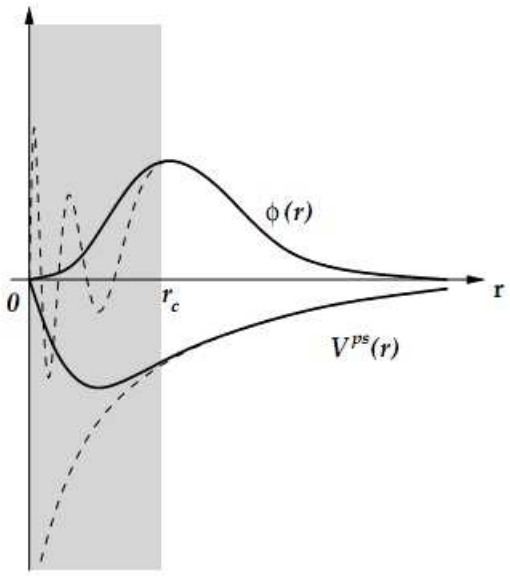

Figure 1.2. Schematic representation of the pseudo-wavefunction $\phi(r)$ and pseudopotential $V^{ps}(r)$; r_c is the cutoff radius beyond which the wavefunction and potential are not affected. Dashed lines indicate real valence wavefunction and Coulomb potential [18].

electrons. This average core effect operator is called an effective core potential (ECP) or a pseudopotential [3].

The advent of ab initio molecular dynamics using the Car-Parrinello (CP) method [19] has resulted in a considerable leap in the capability of planewave based density functional methods. The application of these approaches has permitted the solution of numerous previously intractable problems [20].

A distinction is sometimes made between an ECP and a pseudopotential; the latter term is being used to mean any approach limited to the valence electrons, while the former is sometimes used to designate a simplified pseudopotential corresponding to a function with fewer orbital nodes than the correct functions. However, the terms are usually used interchangeably to designate a nuclei-plus-core electrons potential used with a set of valence functions, and that is what is meant here [3].

The relativistic form of the Schrödinger equation i.e. the Dirac equation, is not commonly used explicitly in molecular calculations, but is instead used to develop

relativistic pseudopotentials [3]. Relativistic effects can begin to become significant for about third-row elements, i.e. the first transition metals. For molecules with these atoms ECPs begin to be useful for speeding up calculations, so it makes sense to take these effects into account in developing these potential operators and their basis functions, and indeed ECPs are generally relativistic. Such ECPs can give accurate results for molecules with third-row and beyond atoms by simulating the electronic relativistic mass increase [3].

Let us separate explicitly the single-particle states into valence and core sets, identified as $|\psi^{(v)}\rangle$ and $|\psi^{(c)}\rangle$ respectively, that satisfies Schrödinger type equations in which external potential due to nucleus and all other electron-electron interactions included. We can define a new set of single-particle valence states as follows [18],

$$|\psi^{(v)}\rangle = |\tilde{\psi}^{(v)}\rangle - \sum_c \langle\psi^{(c)}|\tilde{\psi}^{(v)}\rangle\,|\psi^{(c)}\rangle \tag{1.27}$$

Applying the single-particle hamiltonian H^{sp} to this equation, we obtain

$$H^{sp}\,|\tilde{\psi}^{(v)}\rangle - \sum_c \langle\psi^{(c)}|\tilde{\psi}^{(v)}\rangle\,H^{sp}\,|\psi^{(c)}\rangle = \epsilon^{(v)}\left[\,|\tilde{\psi}^{(v)}\rangle - \sum_c \langle\psi^{(c)}|\tilde{\psi}^{(v)}\rangle\,|\psi^{(c)}\rangle\,\right] \tag{1.28}$$

which takes into account that $H^{sp}\,|\psi^{(c)}\rangle = \epsilon^{(c)}\,|\psi^{(c)}\rangle$ giving,

$$\left[H^{sp} - \sum_c \epsilon^{(c)}\,|\psi^{(c)}\rangle\,\langle\psi^{(c)}|\,\right]|\tilde{\psi}^{(v)}\rangle = \epsilon^{(v)}\left[1 - \sum_c |\psi^{(c)}\rangle\,\langle\psi^{(c)}|\,\right]|\tilde{\psi}^{(v)}\rangle \tag{1.29}$$

reduces

$$\left[H^{sp} + \sum_c \left(\epsilon^{(v)} - \epsilon^{(c)}\right)|\psi^{(c)}\rangle\,\langle\psi^{(c)}|\,\right]|\tilde{\psi}^{(v)}\rangle = \epsilon^{(c)}\,|\tilde{\psi}^{(v)}\rangle\,. \tag{1.30}$$

Therefore, the new states $|\tilde{\psi}^{(v)}\rangle$ obey a single-particle equation with a modified potential, but have the same eigenvalues $\epsilon^{(v)}$ as the original valence states $|\psi^{(v)}\rangle$. The modified potential for these states is called the *pseudopotential*, given by

$$V^{ps} = V^{sp} + \sum_{c} \left(\epsilon^{(v)} - \epsilon^{(c)}\right) |\psi^{(c)}\rangle \langle\psi^{(c)}| \tag{1.31}$$

and, correspondingly, the $|\tilde{\psi}^{(v)}\rangle$'s are called *pseudo-wavefunctions*. And finally the entire procedure of constructing typical pseudopotentials for modern calculations is schematically shown in Figure 1.3.

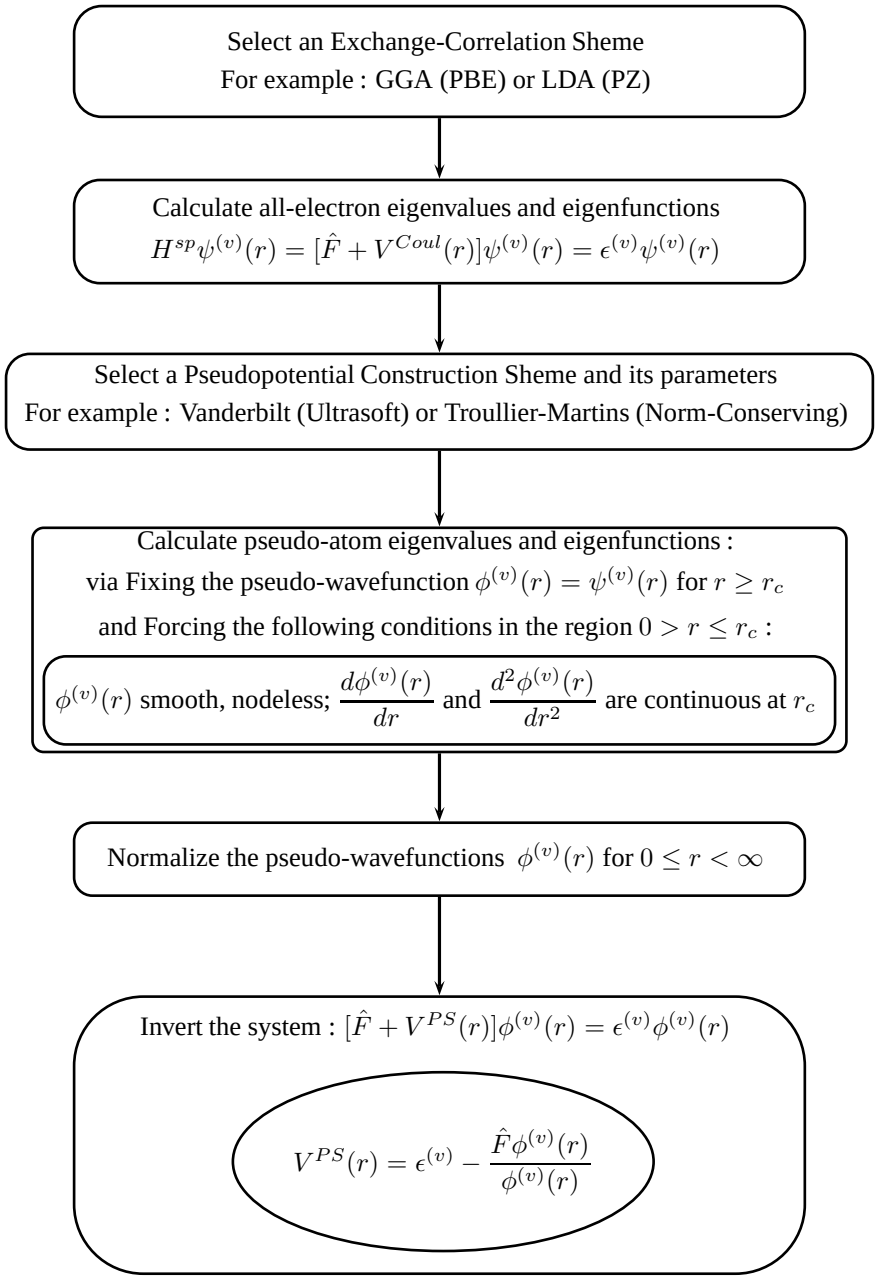

Figure 1.3. Typical pseudopotential construction scheme.

PART 2

HEUSLER STRUCTURE

The compounds which contain magnetic transition elements are grouped in four large classes due to their magneto-optical properties. These comprise spinels, garnets, orthoferrites, and Heusler alloys [21], the last one being the class of materials we are interested in the scope of this thesis.

2.1. HALF METALLICITY AND HEUSLER ALLOYS

The Heusler alloys NiMnSb, PdMnSb, and PtMnSb have been investigated experimentally and theoretically since 1980's [22]. At the time the unusual magneto-optical properties of several Heusler alloys motivated the study of their electronic structure which yielded an unexpected result [22].

Firstly the compound PtMnSb has been found experimentally to have an extremely large magneto-optical Kerr rotation of -1.27° that was the record Kerr rotation observed in a transition metal compound in room temperature and was therefore called a *giant* Kerr effect. Almost simultaneously, the theoretical finding of the so-called *half-metallic* nature of the PtMnSb was reported [21]. The alloy showed the properties of metals as well as insulators at the *same* time in the *same* material, depending on the spin direction. This property was given the name of half-metallic magnetism [23].

More explicitly, half-metallicity means that the material is metallic for majority, but insulating for minority spin electrons according to band structure theory. Such a gap for one spin type naturally may give rise to unusual magnetotransport and optical properties. NiMnSb system was also predicted to be half-metallic, while the PdMnSb was not. The detailed comparison became feasible only due to the development of *ab*

initio calculations of the magneto-optical spectra.

Half-metallic ferromagnets represent a class of materials which attracted a lot of attention due to their possible applications in spintronics (also known as magnetoelectronics) [24]. Adding the spin degree of freedom to the conventional electronic devices has several advantages like non-volatility, increased data processing speed, decreased electric power consumption, and increased integration densities [25–27]. Half-metals can be considered as hybrids between metals and semiconductors.

However the expected 100% spin polarization in a half-metallic ferromagnet is a limit of vanishing temperature and can be achieved by neglecting spin-orbit interactions [22]. The number of well-established half-metals is a confusing situation originating from the fact that there is no direct experiment to determine whether a material is a half-metal or not. Because of experimental complications, electronic structure calculations which are based on DFT in the LDA or GGA play an important role in the search for finding new half-metallic ferromagnets. The power of computational calculations is that it does not need samples, moreover the calculations can be performed for hypothetical materials.

2.2. HEUSLER STRUCTURE AND HALF-METALLICITY

Now we will present a study of the basic electronic and magnetic properties of the half-metallic Heusler alloys. Using *ab-initio* results we explain the origin of the gap in both the half- and full-Heusler alloys [28].

As mentioned above, developments in electronics have brought half-metallic ferromagnets to the center of scientific research recently. The first family of Heusler alloys studied was of the form $\mathrm{X_2YZ}$, in the $\mathrm{L2_1}$ structure, which consists of four fcc sublattices, where X is a high-valence transition or noble metal atom, Y a low-valance transition metal and Z an sp element [29] as shown in Figure 2.1.

Particulary compounds that contain Co and Mn have attracted most of the attention.

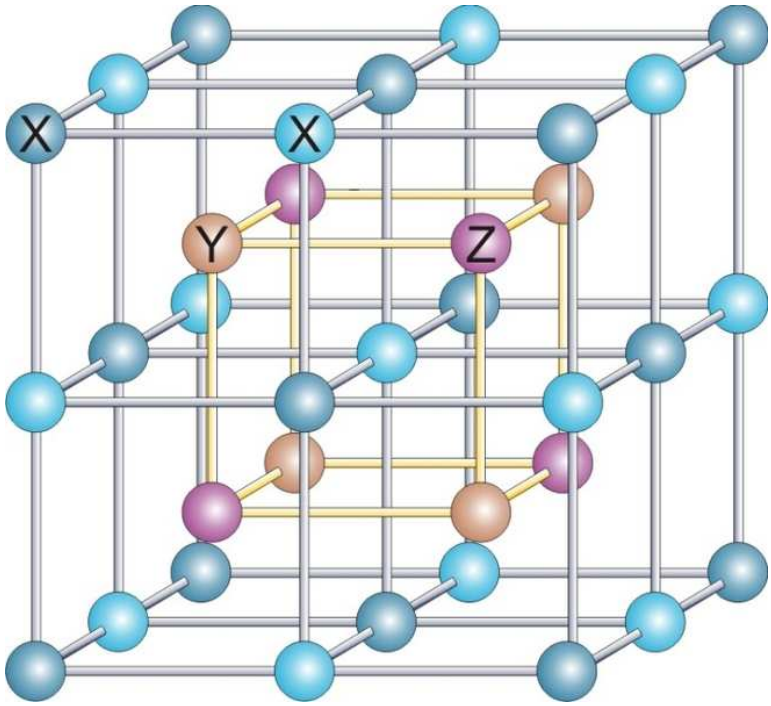

Figure 2.1. X_2YZ, in the $L2_1$ structure.

Each Mn or sp atom has eight Co atoms as first neighbors, sitting on an octahedral symmetry position, while each Co has four Mn and four sp atoms as first neighbors and thus the symmetry of the crystal is reduced to the tetrahedral one. The Co atoms occupying the two different sublattices are chemically equivalent as the environment of the second one but rotated by 90° [28].

The Heusler alloys of the second class are of the form XYZ, in the $\mathrm{C1_b}$ structure, and consisting of three fcc sublattices. They are often called semi- or half-Heusler alloys in the literature, while $L2_1$ structures are referred to as full-Heusler alloys [29]. It can be understood that Heusler $\mathrm{C1_b}$ alloys have a close relation with the zinc-blende structure which has an fcc Bravais lattice with a basis of $(0, 0, 0)$ and $(1/4, 1/4, 1/4)$. The Heusler $\mathrm{C1_b}$ structure consists of the zinc-blende structure with an additional occupation of the $(1/2, 1/2, 1/2)$ site. Heusler $L2_1$ structure differs from the Heusler $\mathrm{C1_b}$ structure with an additional occupation of the $(3/4, 3/4, 3/4)$ site [28].

The structure of full-Heusler system results in the occurrence of an inversion center that is not present in the $\mathrm{C1_b}$ and zinc-blende structures [28]. This difference has important

consequences for the half-metallic band gaps [28]. The interest in these types of intermetallic alloys increased after the prediction of NiMnSb using first-principles calculations.

Heusler alloys have main advantages like high Curie temperatures compared to other half-metallic systems such as oxides and manganites [29]. Heusler alloys have already been incorporated in spin-filters [30], tunnel junctions [31], and giant magneto-resistance (GMR) devices [32]. The most successful recent applications in spintronics concern the half-metallic full-Heusler alloys which are the systems we will investigate in detail for two particular compounds by using first-principles calculations.

2.2.1. Band Structure of Heusler Alloys

In the non-magnetic case, the local contributions to the density of states (DOS) comes from the d-states of X and Y atoms dominantly while the sp-atom introduces deep lying s and p bands. Since all atomic orbitals, i.e. the d and sp orbitals hybridize with each other, all bands are hybrids between these states, being either of bonding or antibonding type [33].

Those configurations is energetically not stable, since the Fermi energy, E_F, lies in the middle of an antibonding band and since the X atom can gain considerable exchange energy by forming a magnetic moment. So that spin polarized results show a different picture in which the majority spin-$\uparrow$ band has X-d states shifted to lower energies forming a common d-band with the Y-d states, while in the minority spin-$\downarrow$ band, the X states are shifted to higher energies and are unoccupied. Therefore a band gap at E_F is formed separating the occupied d bonding from the unoccupied d-type antibonding states which is the case that ensures XYZ is a half metal, with a band gap at E_F in the minority band and a metallic sp-like DOS at E_F in the majority band [33].

The band structure of the half-Heusler alloys due to minority states is important for the understanding of the magnetic properties, and this band structure is universally valid for all half-Heusler alloys including the semiconductors [33].

It can easily be understood that the gap is dominated by d-states and originates from the strong hybridization between the d-states of the two transition metal atoms. Note that in the $\mathrm{C1_b}$ structure, X and Y sublattices form a zinc-blende type structure, which is important for the formation of the gap [33].

Half-metallic $\mathrm{C1_b}$ compounds have a gap which is normally indirect, with maximum of the valence band at the Γ point and the minimum of the conduction band at the X point. It will be seen for two particular compounds that the band gap can be well described by the LDA and GGA since the screening is metallic in these systems [33].

If we look at the role of the sp-elements, it is clear that they are not responsible for the existence of the band gap, but they are nevertheless very important for the physical properties of the Heusler alloys and the structural stability of $\mathrm{C1_b}$ structure.

The second family of Heusler alloys, which will be discussed more deeply for two particular compounds in the next section, are the full-Heusler alloys. The importrance of the full-Heusler alloys which are all strong ferromagnets is that they have high Curie temperatures above $600\,\mathrm{K}$ and they show very little disorder except for the $\mathrm{Co_2MnAl}$ compound. Similar to the half-Heusler alloys, sp bands are not relevant for the band gap and located far below the E_F. Therefore, only the hybridization of one Y and two X atoms can be considered as the reason of the gap. For simplicity, only the d-states at the Γ point can be considered, which show the full structural symmetry. We note that X atoms form a simple cubic lattice and the Y atoms that have 8 X atoms as the nearest neighbor, occupy the body centered sites. The distance between the X atoms is a second neighbor distance but the hybridization between the X atoms qualitatively very important because of field splitting due to simple cubic lattice formed by X atoms.

In a second step the hybridization between X-X orbitals and Y-d orbitals can be considered. They create a doubly degenerate bonding state that is very low in energy and an anti-bonding one that is unoccupied and locates above the E_F [33]. The origin of the band gap in the full-Heusler alloys is rather subtle.

2.2.2. Slater-Pauling Behavior

The total magnetic moment in units of Bohr magneton (μ_B) is just the difference between the number of occupied spin-$\uparrow$ states and occupied spin-$\downarrow$ states. The number of spin-down bands below the gap is $N_\downarrow = 9$ in all cases. If the total number of valence electrons is Z_t we deduce the number of occupied spin-up states $N_\uparrow = Z_t - N_\downarrow = Z_t - 9$ and the total magnetic moment is found to be $M = (N_\uparrow - N_\downarrow)\mu_B = (Z_t - 18)\mu_B$. For example in the NiMnSb, we have $N_\uparrow = 13$ and $M = 4\mu_B$. It will be seen that the calculated local moment per unit cell by the ab-initio methods will be very close to the characteristic value for half-metallic full-Heusler alloys. This is a direct analogue to the well-known Slater-Pauling behavior of the binary transition metal alloys [34] with a difference of minority population which is fixed and equal to 9, so that the screening is achieved by filling the majority band.

It seems in full-Heusler alloys the total spin moment, M_t, is related to the total number of valence electrons, Z_t, with a similar equation of the half-Heusler alloys. The behavior is shown in Figure 2.2. Minority band contains 12 electrons per unit cell, i.e. $N_\downarrow = 12$. So that, we immediately arrive that $M_t = Z_t - 24$ where Z_t is total number of valence electrons. Overall it is seen that many the results coincide with the Slater-Pauling curve.

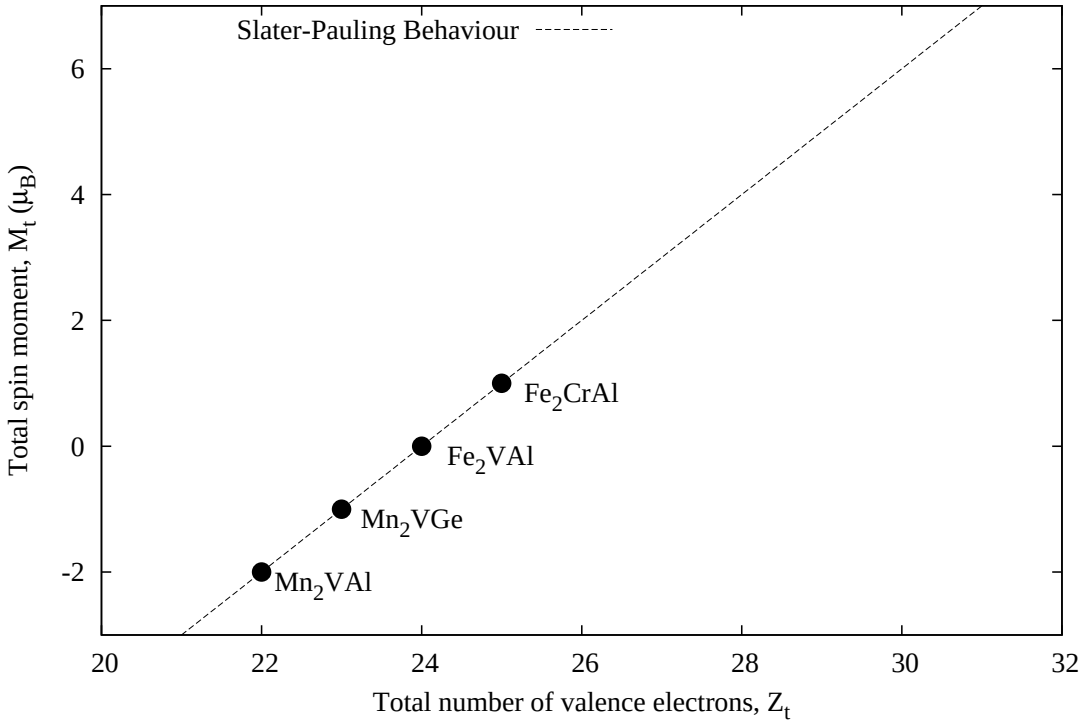

Figure 2.2. Slater-Pauling behavior in full-Heusler systems with some examples.

PART 3

SYSTEMS UNDER INVESTIGATION

Half-metallic ferromagnets (HMFs) have attracted great attention due to their extraordinary physical properties and several technological applications in various fields. NiMnSb half-Heusler compound is the firstly discovered half-metallic ferromagnet with $\mathrm{C1_b}$ structure and $\mathrm{F43m}$ space group [23]. HMFs are characterized by the metallic band structure for one spin state, while the electronic band structure of other spin state presents an insulating character yielding a perfect spin polarization at E_F. This situation also results in a spin-polarized electrical conductivity, which is very sensitive to applied magnetic field. HMFs have central importance in spin-dependent electronic applications: spintronics [24, 35], GMR spin valve [36], and spin injection to semiconductors [37–39].

These types of materials have been extensively studied in view of the first principles calculations, and several compounds are predicted to be half-metallic [22, 40–44]. The electronic structure and magnetic properties of half- and full-Heusler compounds with various combinations of constituent elements have been studied extensively in previous works [45, 46]. A recent comprehensive ab initio study reviews the electronic structure and spin polarization properties of half-metallic Heusler alloys [47]. Among the several Co-based full-Heusler compounds ($\mathrm{Co_2YZ}$) in cubic $\mathrm{L2_1}$ structure, $\mathrm{Co_2MnSi}$ system seems to be the most promising material for spintronics applications due to the ideal physical properties like high Curie temperature ($T_c = 985K$) [48] and wide band gap in minority spin channel [44]. Co-based Heusler compounds are investigated theoretically in view of the density functional calculations and most of them are predicted to be half-metallic [42–45, 48–50]. Moreover, $\mathrm{Co_2MnSi}$ compound is used in production of thin films [51–53] and devices [54, 55].

The half-metallic behavior of full-Heusler compounds presents more complicated characteristics than that of half-Heusler alloys due to the presence of the states located entirely at the Co sites [45, 56] resulting an ideal local moment system [57, 58]. The integer magnetic moment is an important characteristic property for half-metallic systems in stoichiometric composition. The total magnetic moments of the perfect HMFs obey Slater-Pauling [59, 60] rule, in which the saturation magnetic moment scales with the number of valance electrons [61]. Besides CoMn based full-Heusler compounds, there is a lack of study in literature on CoCr based Heusler systems. In this thesis, the electronic structure and magnetic properties of two novel full-Heusler compounds, $\mathrm{Co_2CrAs}$ and $\mathrm{Co_2CrSb}$, are investigated using plane-wave pseudopotential method and spin-polarized GGA (σ-GGA) of DFT. There are no comparable studies on electronic structure and half-metallicity of these systems in literature. The details of the calculations performed and Heusler geometry are described in next section. The features of bulk $\mathrm{L2_1}$ structures of the compounds under study are also presented in next section.

PART 4

COMPUTATIONAL DETAILS

Materials that have been investigated in our study were the full-Heusler ternary intermetallic compounds, Co_2CrAs and Co_2CrSb, based on the X_2YZ stoichiometry for the $L2_1$ phase ($Fm\bar{3}m$ space group, $\#225$) including one formula unit of atoms per primitive cell.

X atoms are transition metals located at $(0, 0, 0)$ and $(\frac{1}{2}, \frac{1}{2}, \frac{1}{2})$ Wyckoff crystallographic positions, while Y and Z are a magnetic transition metal and a III-V group element occupying the positions $(\frac{1}{4}, \frac{1}{4}, \frac{1}{4})$ and $(\frac{3}{4}, \frac{3}{4}, \frac{3}{4})$, respectively. These are the materials that show ferromagnetic behavior even though none of the atoms in the composition is ferromagnetic, which is the phenomena that makes them important.

All the calculations that will be presented in this work have been carried out by using PWscf code, distributed with the Quantum ESPRESSO package [62, 63]. In order to approximate exchange correlation potential, σ-GGA of the density functional theory [8, 9] is used with Perdew-Burke-Ernzerhof parametrization [16].

In describing the physical properties of Heusler compounds, GGA functionals are more successful than local spin density functional (LSDA) scheme [43]. Ultrasoft pseudopotentials are generated by scalar relativistic calculation for all the atoms in the composition with non-linear correction. The valence states of atoms are considered as follows, Co: $4s^1 3d^8$, Cr: $3s^2 3p^6 4s^1 3d^5$, As: $4s^2 4p^3$, Sb: $4d^{10} 5s^2 5p^3$. An automatically generated $20x20x20$ k-point grid following the convention of Mankhorst and Pack [64] is used for Brillouin zone integration yielding 512 k-points in the irreducible wedge of the Brillouin zone centered at Γ point.

Wave functions are expanded in plane wave basis sets up to a kinetic energy cut-off value of $50\,\mathrm{Ry}$ corresponding to about 1940 plane waves. The electron kinetic energy cut-off value has been determined by calculating the total energies at different kinetic energy cut-off values as given in Figure 4.1–4.2. The convergence is well provided with $50\,\mathrm{Ry}$ cut-off value which is sufficient for ultrasoft pseudopotentials used in calculations. The observed total energy difference between $50\,\mathrm{Ry}$ and $90\,\mathrm{Ry}$ cut-offs is approximately $7\,\mathrm{mRy}$ for both systems studied indicating a well-converged ground state.

Mathfessel-Paxton type smearing with parameter $\sigma = 0.005\,\mathrm{Ry}$ is applied on fermionic occupation function [65], and Davidson type diagonalization method [66] with $10^{-8}\,\mathrm{Ry}$ energy convergence threshold was used in order to solve KS equations iteratively. In order to get equilibrium structural parameters of the systems, we use Vinet equation of state [67] which is found to be most accurate among the several equation of state formulations [68]. This formulation is as follows:

$$E(V,T) = E_0(T) + \frac{9B_0(T)V_0(T)}{\chi^2}\left[1 + \left[\chi(1-x) - 1\right]e^{\chi(1-x)}\right] \tag{4.1}$$

in which $x = (V/V_0)^{1/3}$ and $\chi = 3(B_0' - 1)/2$, where V_0 is the equilibrium volume, B_0 is zero pressure bulk modulus and B_0' is its pressure derivative. We construct the static equation of states of the system performing fits using the total energies at 20 different volumes ranging from $0.8V_0$ to $1.2V_0$.

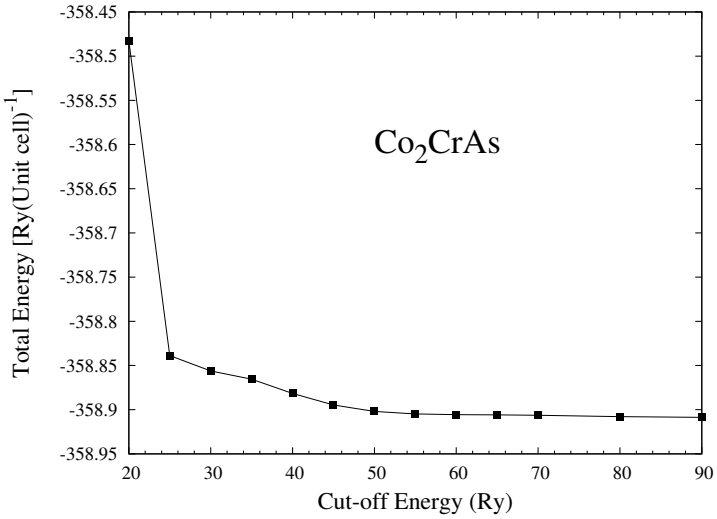

Figure 4.1. Energy cut-off test for Co_2CrAs.

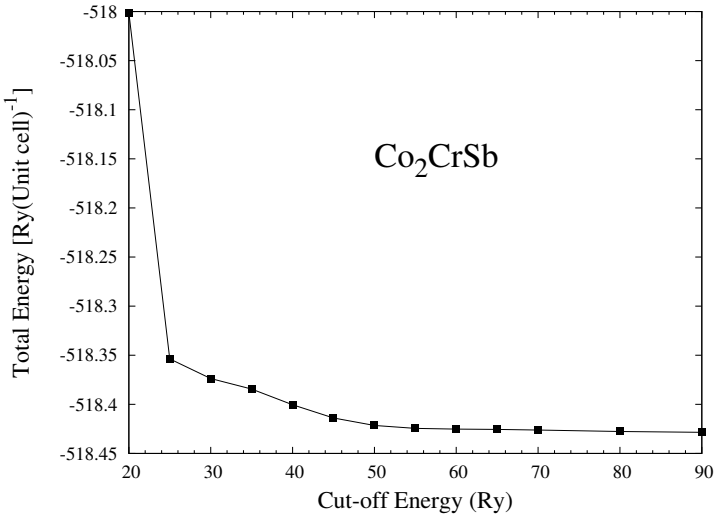

Figure 4.2. Energy cut-off test for Co_2CrSb.

PART 5

RESULTS AND DISCUSSION

While studying the half-metallic systems, the accurate determination of equilibrium structural parameters has central importance, since the electronic band structure is sensitive to applied strain. We show the calculated total energies as a function of lattice constant together with the fitting curves for the relevant systems in Figure 5.1 and 5.2. The asymptotic standard errors in fitting curves are less then 10^{-6} which shows the precision of the obtained results. A summary of calculated structural parameters of $\mathrm{Co_2CrAs(Sb)}$ systems is given in Table 1 showing equilibrium lattice parameters in $\mathrm{a.u.}$, Bulk moduli in GPa, and magnetic moments in μ_B.

Table 5.1. Equilibrium structural parameters of bulk $\mathrm{Co_2CrX\,(X = As,\ Sb)}$

	$\mathrm{Co_2CrAs}$	$\mathrm{Co_2CrSb}$
a (a.u.)	10.933	11.322
B (GPa)	179.3	173.9
μ_{tot} (μ_B)	5.00	5.00
μ_{Co} (μ_B)	1.98	1.92
μ_{Cr} (μ_B)	2.95	3.13
$\mu_{As(Sb)}$ (μ_B)	0.07	-0.05

The calculated lattice constant is $10.933\,(11.322)$ a.u., the zero pressure bulk moduli is $179.3\,(173.9)\,GPa$ for the system $\mathrm{Co_2CrAs(Sb)}$. These values are relatively low compared to $\mathrm{Co-Mn}$ based Heusler systems. (e.g. $B_0 = 214$ GPa for $\mathrm{Co_2MnSi}$ [69]).

The calculated equilibrium lattice constants of several full- and half-Heusler systems using $\sigma - \mathrm{GGA}$ deviate from experimental results by a ratio of 1% following general tendency of $3\mathrm{d}$ elements [43] corresponding to large improvement over $\mathrm{L(S)DA}$. Thus, it is deduced that $\sigma - \mathrm{GGA}$ scheme can be used to obtain accurate results.

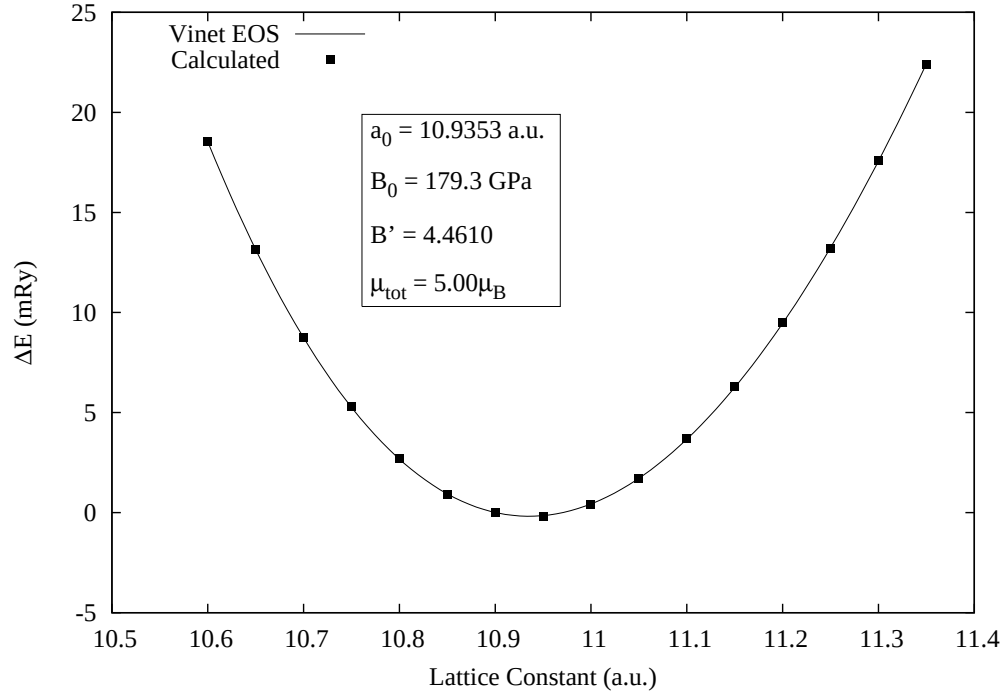

Figure 5.1. Static equation of states of Co_2CrAs with calculated data and fitting curve.

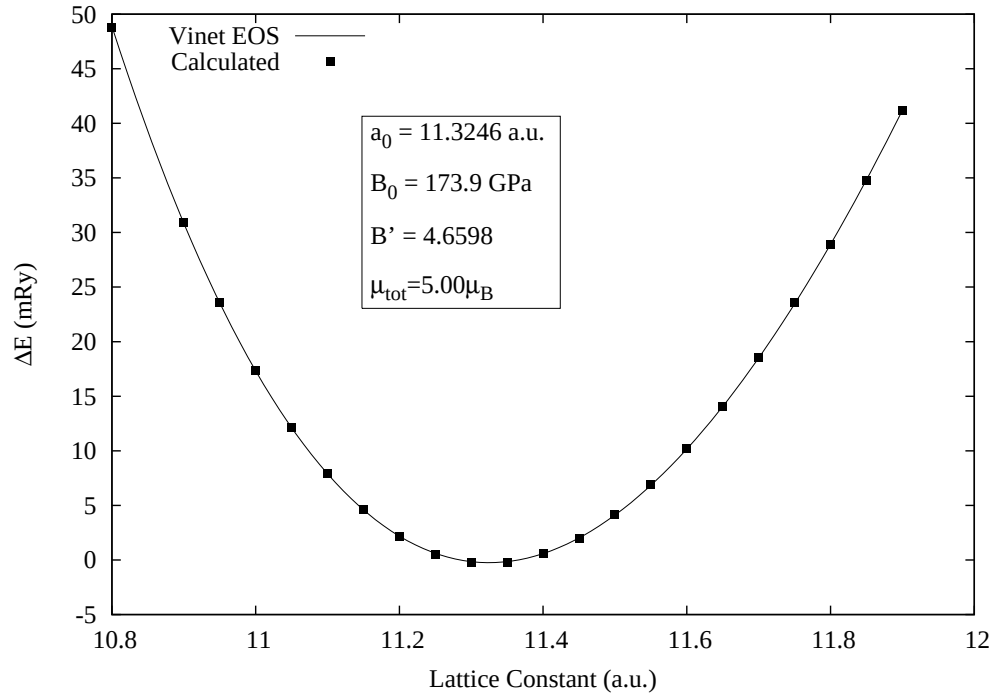

Figure 5.2. Static equation of states of Co_2CrSb with calculated data and fitting curve.

One of the properties of the half-metallic systems that indicate the stability of behavior is the total magnetic moment which is found to be an integer $5.00\mu_B$ obeying the Slater-Pauling rule with the number of valence electrons $Z_t = 29$ for both Co_2CrAs and Co_2CrSb systems in cubic $L2_1$ structure. The largest contributions to total magnetic moments are due the chromium site with the value $2.95(3.13)\mu_B$ for the compound $Co_2CrAs(Sb)$, while the magnetic moments of the sp elements show relatively large difference with the value $0.07(-0.05)\mu_B$ for $As(Sb)$.

It is realized that the calculation conditions affect the sensitivity of the magnetic moments. A relatively weaker Brillouin zone integration with 15x15x15 k-mesh and increased smearing parameter (e.g. 0.02 Ry) give non-integer saturation magnetic moments.

The GGA calculated spin resolved electronic band structures of the $Co_2CrAs(Sb)$ systems along the main symmetry directions in irreducible Brillouin zone and the total electronic DOS are given in Figure 5.3–5.8.

Electronic bands of the majority spin states show typical metallic character with bands crossing E_F in all high symmetry directions, while the band structures of the minority states show semiconducting behavior with the energy band gaps $E_{gap} = 0.40\,\mathrm{eV}$ and $E_{gap} = 0.46\,\mathrm{eV}$ for Co_2CrAs and Co_2CrSb systems, respectively. The minority spin band structures show direct gap at Γ point for Co_2CrAs and an indirect gap along $\Gamma - X$ direction for Co_2CrSb. The nature of the minority gap is also very sensitive to calculation conditions.

The difference between the valence band maximum (VBM) and E_F is defined as spin gap which is an important quantity corresponding to the required energy to flip a minority spin from VBM to majority spin E_F [43]. The calculated spin gap values are $E_{spin} = 0.39(0.25)\,\mathrm{eV}$ for $Co_2CrAs(Sb)$. The increasing atomic number of sp elements in composition results in a reduced spin gap value.

The orbital projected spin-resolved electronic DOS (EDOS) shown in Figure 5.9–5.10

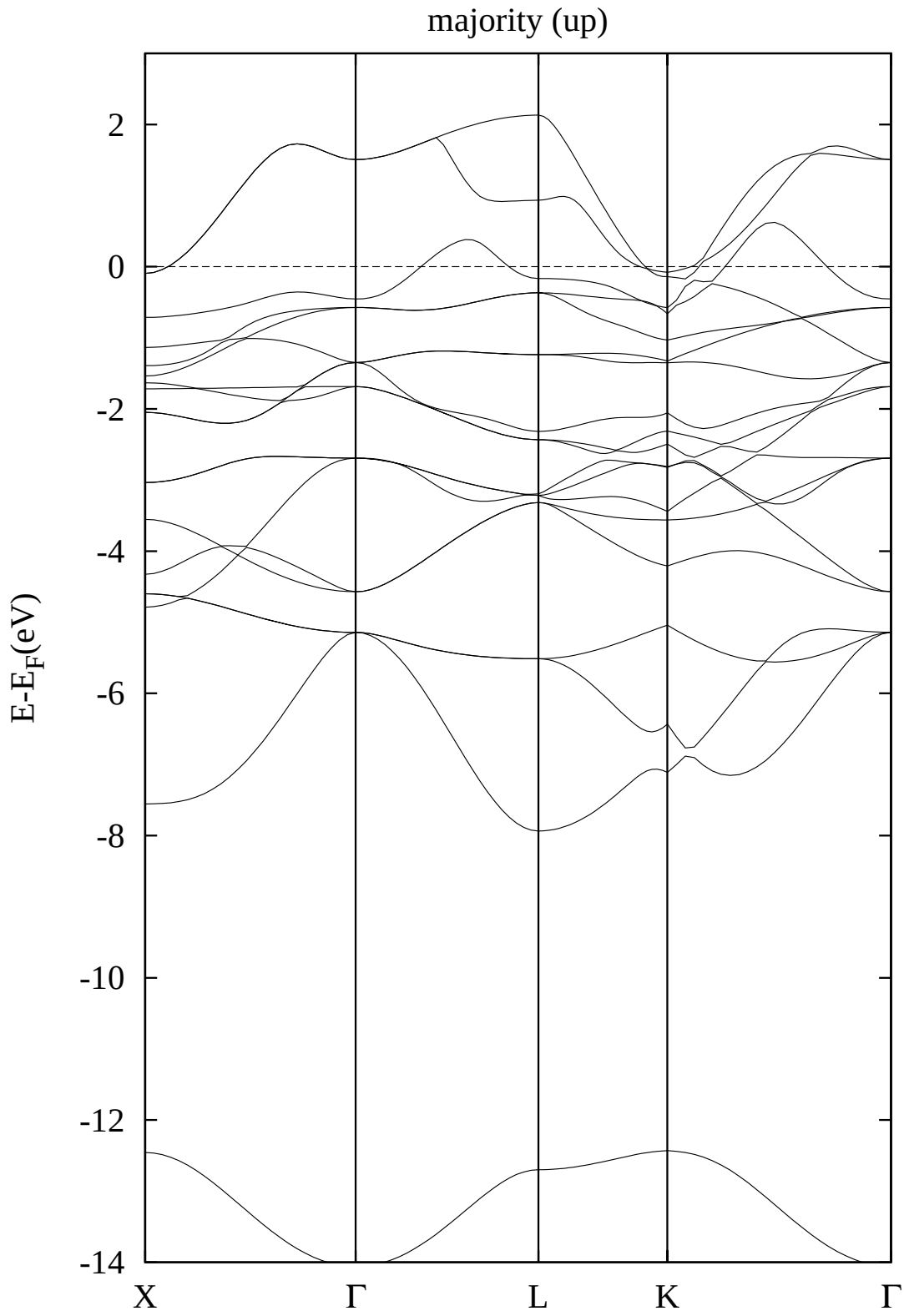

Figure 5.3. Spin resolved electronic band structure of bulk Co_2CrAs for majority spin-↑ states at equilibrium. E_F was set to zero.

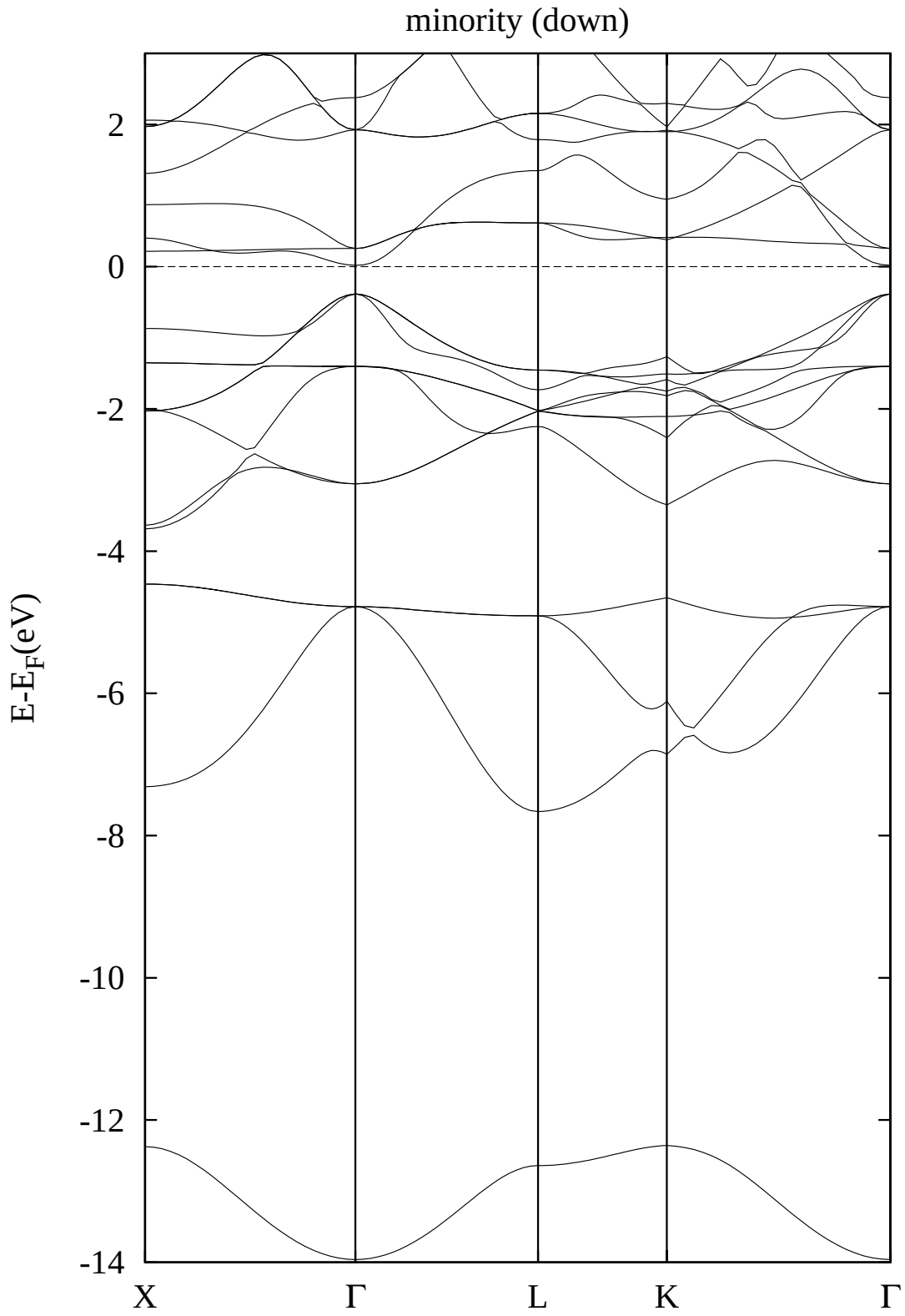

Figure 5.4. Spin resolved electronic band structure of bulk Co_2CrAs for minority spin-$\downarrow$ states at equilibrium. E_F was set to zero.

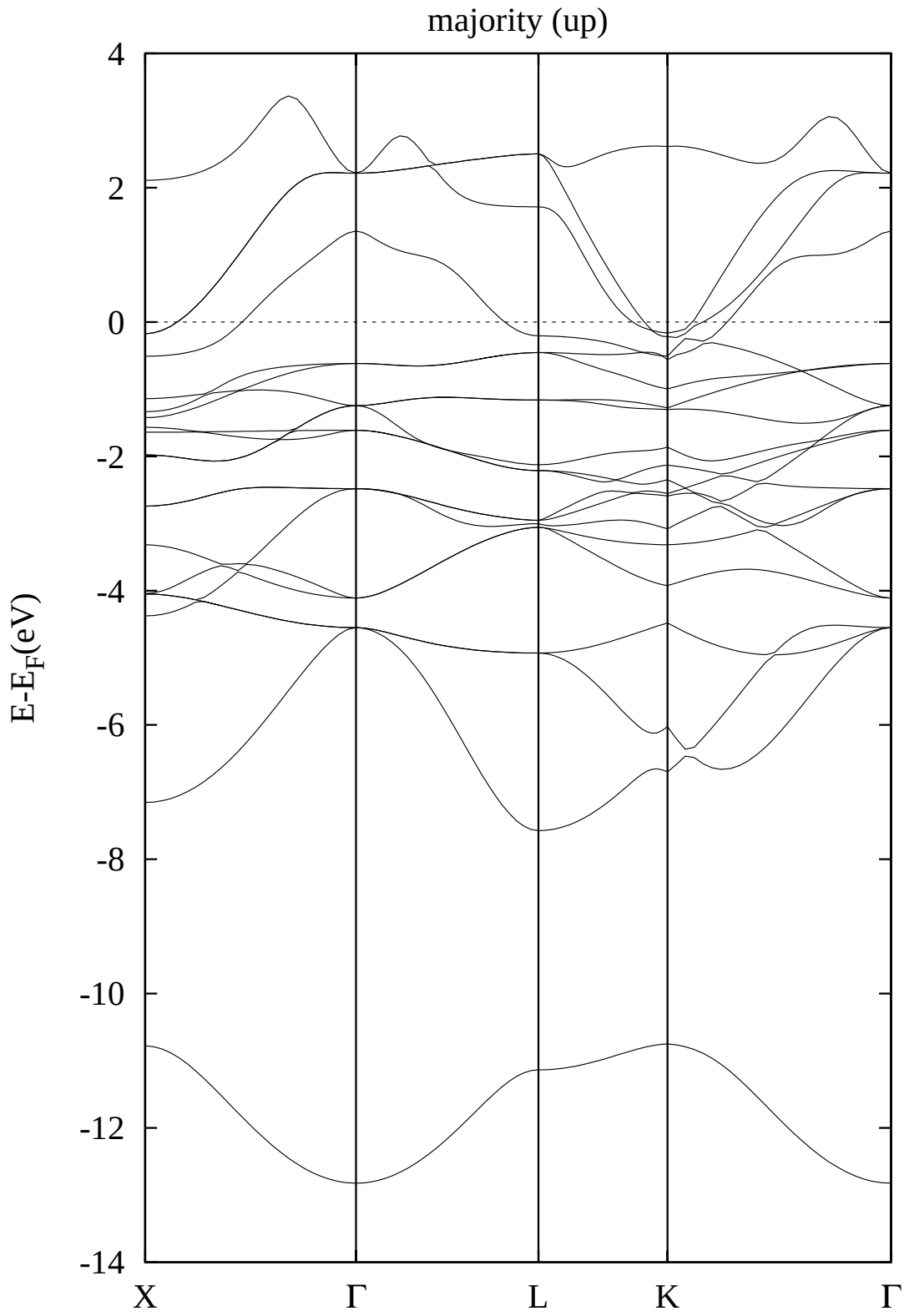

Figure 5.5. Spin resolved electronic band structure of bulk Co_2CrSb for majority spin-↑ states at equilibrium. E_F was set to zero.

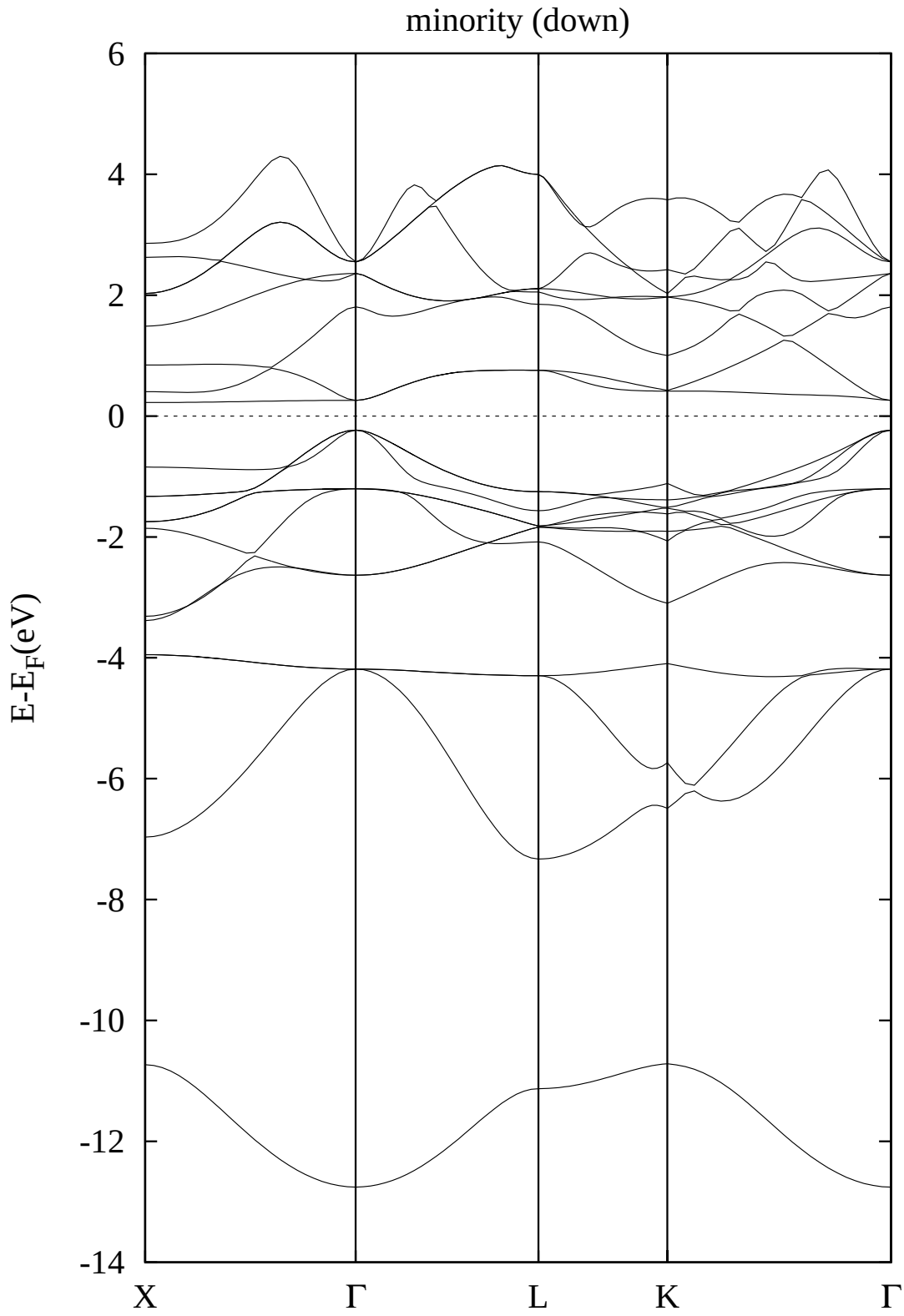

Figure 5.6. Spin resolved electronic band structure of bulk Co_2CrSb for minority spin-$\downarrow$ states at equilibrium. E_F was set to zero.

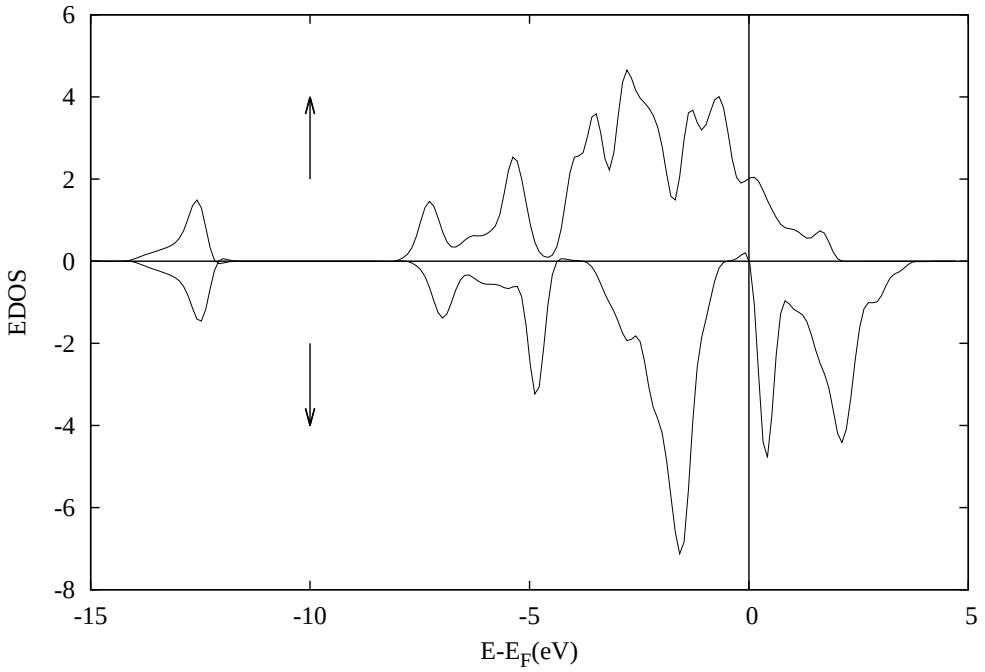

Figure 5.7. Spin resolved total EDOS of bulk Co_2CrAs. E_F was set to zero.

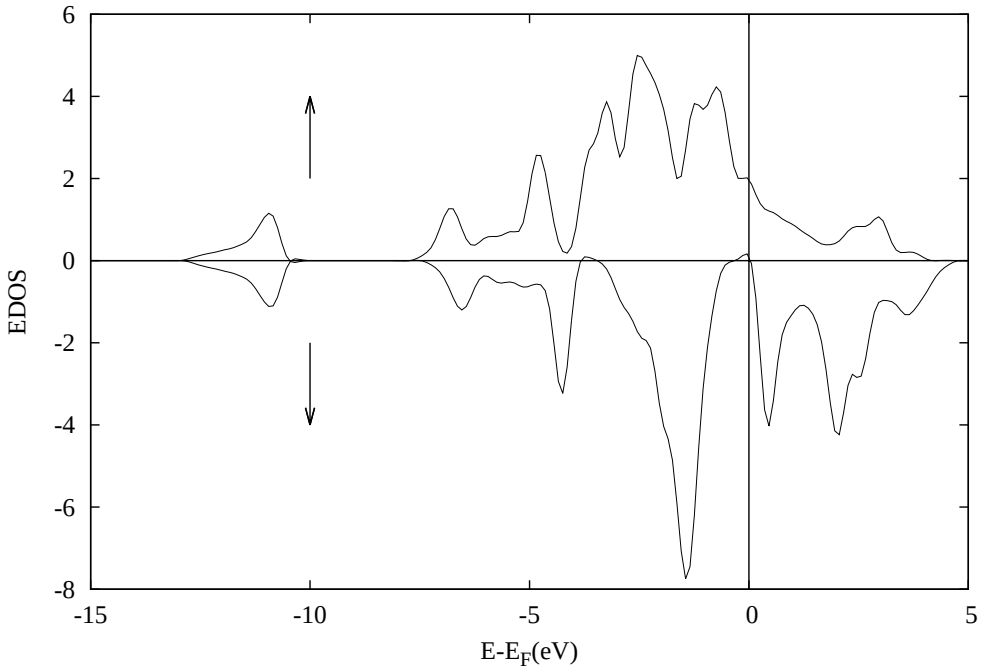

Figure 5.8. Spin resolved total EDOS of bulk Co_2CrSb. E_F was set to zero.

give a sensible understanding of the systems. Deep lying energy bands around $-12\,\mathrm{eV}$ and $-14\,\mathrm{eV}$ are due to the p-states of chromium atom and are not strongly affected by the interaction of $3\mathrm{d}$-states of cobalt and chromium atoms. The bands around $-7\,\mathrm{eV}$ are mainly caused by the p-states of group-V sp elements $\mathrm{As(Sb)}$. For both spin configurations, d-states of cobalt and chromium sites show their dominant character between $-5\,\mathrm{eV}$ and $-4\,\mathrm{eV}$ energy range. The majority bands around the E_F results from the strong hybridization of d-states of cobalt and chromium atoms while the the minority spin energy band gap around E_F is restricted by d-states of cobalt atoms. This gap is originated from the interactions of d-states of cobalt atoms standing on two different atomic positions as expected in Co-based full-Heusler systems [40]. Spin-resolved electronic band structures together with total EDOS are also given in Figure 5.11–5.12.

We can easily state that both valence and conduction bands of minority spin states around $\pm 2\,\mathrm{eV}$ of the E_F emerge from the hybridization of Co-d-states. $3\mathrm{d}$ orbitals of Co atoms couple and form bonding hybrids [22]. Consequently, the minority band gaps in these systems are due to the bonding and anti-bonding features of Co-d-states. Cr-d-states of minority spins take place at $\approx\ 2\,\mathrm{eV}$ above the E_F with local and non-hybridized character. It should be noted that E_F does not take place at the mid of the minority gap.

The formation enthalpy is a measure of synthesizability of the relevant compounds and can be calculated by using following relation,

$$\Delta H = E(\mathrm{Co_2CrX}) - [E(\mathrm{Co}) + E(\mathrm{CrX})] \tag{5.2}$$

where $E(Co_2CrX)$ is the equilibrium energy of the compound in $\mathrm{L2_1}$ phase, $E(\mathrm{Co})$ and $E(\mathrm{CrX})$ are the energies of the hexagonal close-packed solid cobalt structure containing two atoms per primitive cell and conventional zincblende phase of CrX binary compound, respectively. It is more reasonable to consider the stability of the systems against phase segregation into stable compounds like solid Co and CrX which can occur in sample preparation.

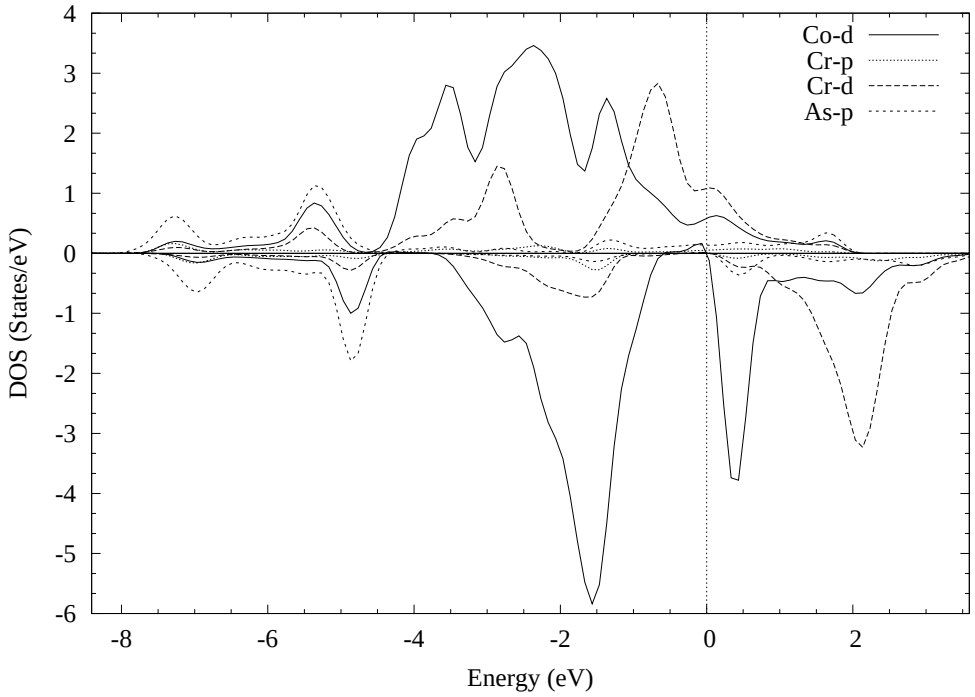

Figure 5.9. Spin-resolved orbital projected EDOS of bulk Co_2CrAs.

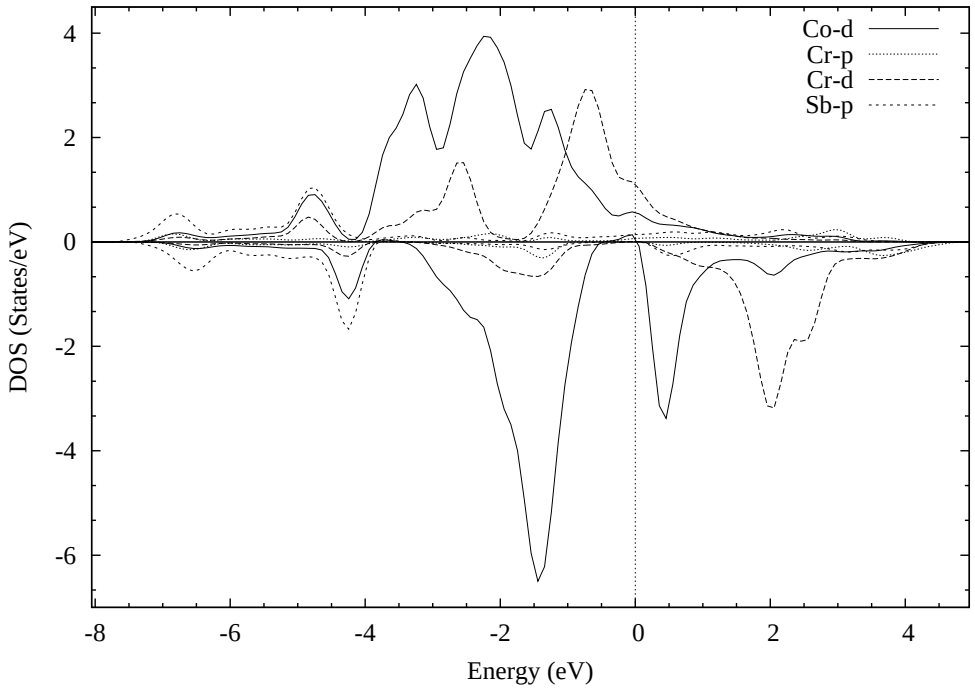

Figure 5.10. Spin-resolved orbital projected EDOS of bulk Co_2CrSb.

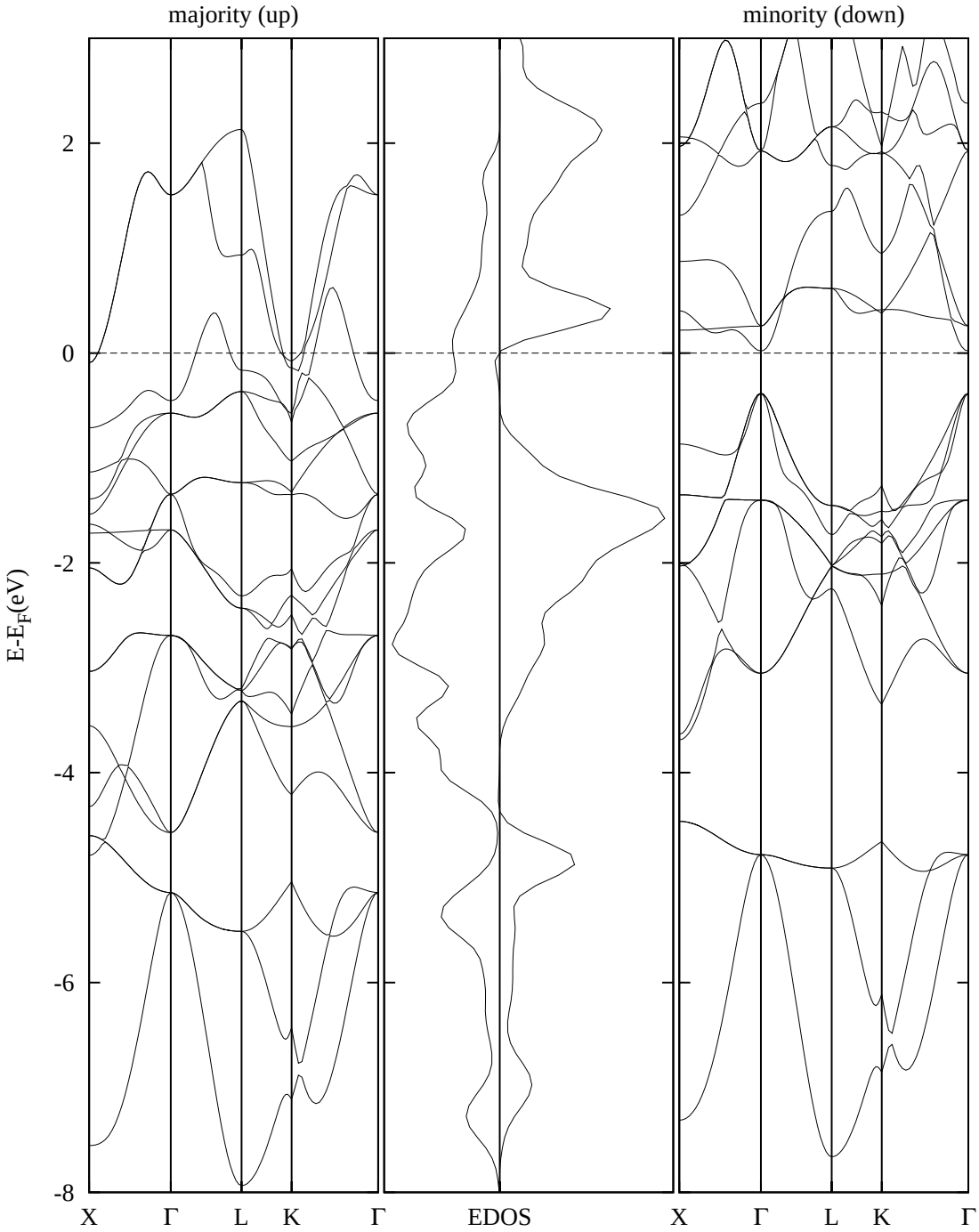

Figure 5.11. Spin-resolved electronic band structure together with total EDOS of bulk Co_2CrAs.

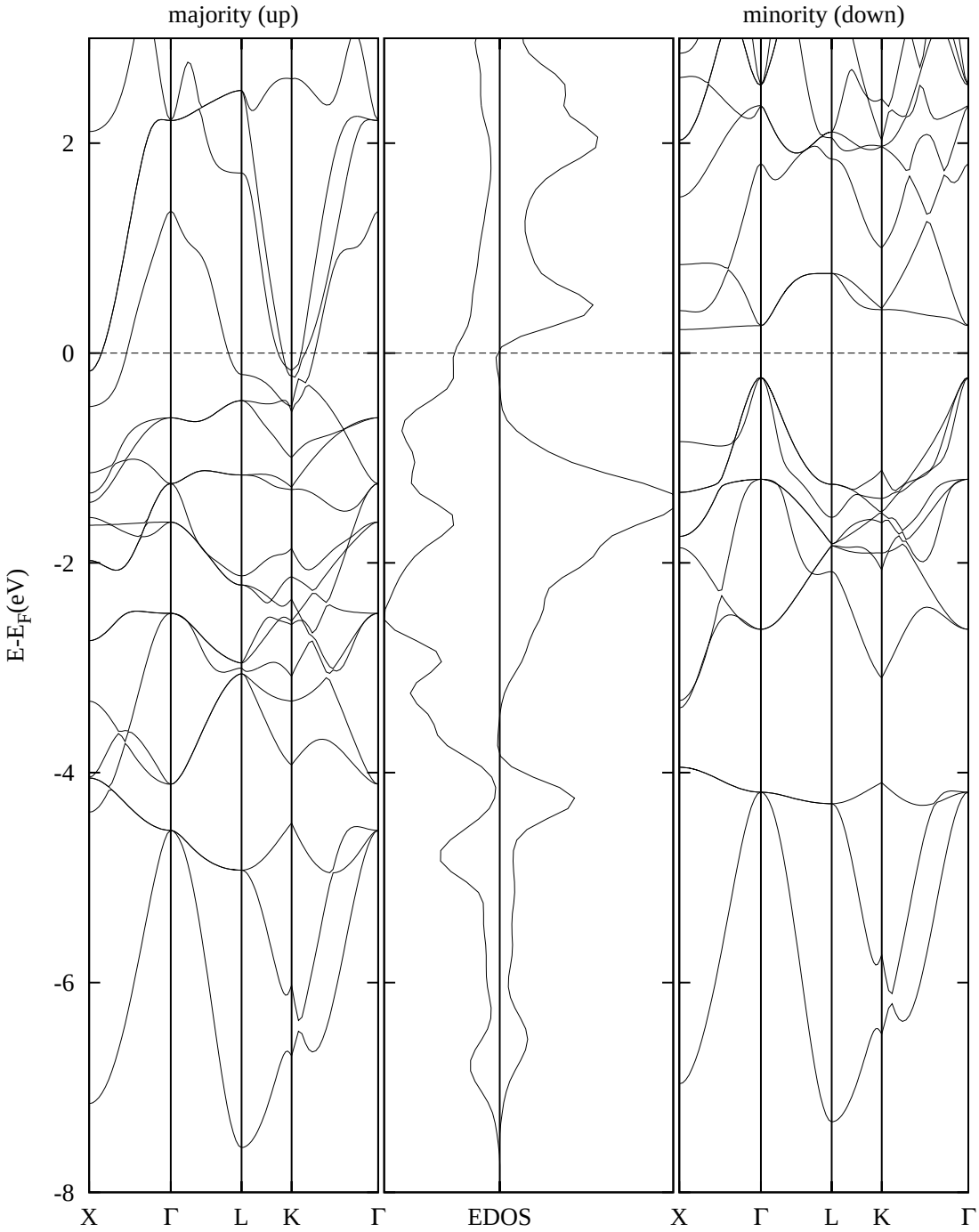

Figure 5.12. Spin-resolved electronic band structure together with total EDOS of bulk Co_2CrSb.

As mentioned above negative values of formation enthalpy is a measure of the stability of the compounds against decomposition into stable solid structures [70]. The calculated enthalpies are $-26.10\,\mathrm{mRy}$ and $-75.09\,\mathrm{mRy}$ for $\mathrm{Co_2CrAs}$ and $\mathrm{Co_2CrSb}$, respectively.

PART 6

SUMMARY AND CONCLUSION

The electronic structure and magnetism of two novel half-metallic full-Heusler compounds, $\mathrm{Co_2CrAs}$ and $\mathrm{Co_2CrSb}$, are studied in the ordered $\mathrm{L2_1}$ structure in view of the first principles density functional calculations. The plane-wave pseudopotential method and spin-polarized GGA scheme for the exchange correlation functionals are applied. These systems show perfect half-metallic character i.e. a semiconducting minority spin band structure, which has zero electronic density of states at Fermi level, and an ordinary metallic band structure for majority spins.

The energy gap in minority spin channel of $\mathrm{Co_2CrAs}$ is found to have a direct gap at Γ-point, while $\mathrm{Co_2CrSb}$ system has an indirect gap along Γ–X direction. The total magnetic moments of both systems are $5.00\mu_B$ in consistet with the Slater-Pauling rule indicating a stable hallf-metallic behavior.

The minority spin energy band gaps are restricted by the d-states of cobalt atoms and it can be inferred that the physical origin of the band gap in minority spin channel is the interactions of the d-states of cobalt atoms at two different sublattices namely $(\mathrm{Co}^1(000) - \mathrm{Co}^2(\frac{1}{2}\frac{1}{2}\frac{1}{2}))$. The calculated formation enthalpies are negative indicating stability and synthezability of these compounds.

REFERENCES

1. Engel, E. and Dreizler, R. M., “Density functional theory: an advanced course”, ***Springer***, New York, 1 (2011).
2. Levine, I. N., “Quantum chemistry 5th ed.”, ***Prentice Hall***, New York, 480 (1999).
3. Lewars, E. G., “Computational chemistry introduction to the theory and applications of molecular and quantum mechanics 2nd ed.”, ***Springer***, New York, 61, 251, 252, 445, 448 (2011).
4. Richard, M. M., “Electronic structure: basic theory and practical methods”, ***Cambridge University Press***, United Kingdom, 5, 201 (2004).
5. Koch, W. and Max, C. H., “A chemist’s guide to density functional theory 2nd ed.” ***Wiley***, Germany, 30 (2001).
6. Slater, J. C., “A simplification of the Hartree-Fock method”, ***Phys. Rev.***, 81 (3): 385–390 (1951).
7. Eschrig, H., “The fundamentals of density functional theory” ***Teubner***, Stuttgart, 74 (1996).
8. Hohenberg, P. and Kohn, W., “Inhomogeneous electron gas”, ***Phys. Rev.***, 136 (3B): B864–B871 (1964).
9. Kohn, W. and Sham, L. J., “Self-consistent equations including exchange and correlation effects” ***Phys. Rev.***, 140 (4A): A1133–A1138 (1965).
10. Parr, R. G. and Yang, W., “Density-functional theory of atoms and molecules”, ***Oxford University Press***, New York, 143 (1989).
11. Vosko, S. H., Wilk, L. and Nusair, M., “Accurate spin-dependent electron liquid correlation energies for local spin density calculations: a critical analysis”, ***Canadian Journal of Physics***, 58 (8): 1200–1211 (1980).
12. Perdew, J. P. and Wang, Y., “Accurate and simple analytic representation of the electron-gas correlation energy”, ***Phys. Rev. B***, 45 (23): 13244–13249 (1992).
13. Becke, A. D., “Density functional calculations of molecular-bond energies”, ***J. Chem. Phys.***, 84 (8): 4524–4529 (1986).
14. Perdew, J. P., “Density-functional approximation for the correlation-energy of the inhomogeneous electron-gas”, ***Phys. Rev. B***, 33 (12): 8822–8824 (1986).
15. Lacks, D. J. and Gordon, R. G., “Pair interactions of rare-gas atoms as a test of exchange-energy-density functionals in regions of large density gradients”, ***Phys. Rev. A***, 47 (6): 4681–4690 (1993).

16. Perdew, J. P., Burke, K. and Ernzerhof, M., “Generalized gradient approximation made simple”, ***Phys. Rev. Lett.***, 77 (18): 3865–3868 (1996).

17. Lee, C., Yang, W. and Parr, R. G., “Development of the Colle-Salvetti correlation-energy formula into a functional of the electron density”, ***Phys. Rev. B***, 37 (2): 785–789 (1988).

18. Kaxiras, E., “Atomic and electronic structure of solids”, ***Cambridge University Press***, New Yok, 72–74, 77 (2003).

19. Car, R. and Parrinello, M., “Unified approach for molecular-dynamics and density-functional theory”, ***Phys. Rev. Lett.***, 55 (22): 2471–2474 (1985).

20. Singh, D. J. and Nordström, L., “Planewaves, pseudopotentials and the LAPW method 2nd ed.”, ***Springer***, USA, 23 (2005).

21. Antonov, V., Harmon, B. and Yaresko A., “Electronic structure and magneto-optical properties of solids”, ***Kluwer Academic Publishers***, Dordrecht, 71, 127 (2004).

22. Katsnelson, M. I., Irkhin V. Y., Chioncel, L., Lichtenstein, A. I. and de Groot, R. A., “Half-metallic ferromagnets: from band structure tomany-body effects”, ***Rev. Mod. Phys.***, 80 (2): 315–378 (2008).

23. de Groot, R. A., Mueller, F. M., Van Engen, P. G. and Buschow, K. H. J., “New class of materials: half-metallic ferromagnets”, ***Phys. Rev. Lett.***, 50 (25): 2024-2027 (1983).

24. Žutić, I., Fabian, J. and Das Sarma S., “Spintronics: fundamentals and applications”, ***Rev. Mod. Phy.***, 76 (2): 323–410 (2004).

25. Wolf, S. A., Awschalom, D. D., Buhrman, R. A., Daughton, J. M., von Molnr, S., Roukes, M. L., Chtchelkanova, A. Y. and Treger, D. M., “Spintronics: a spin-based electronics vision for the future”, ***Science***, 294 (5546): 1488–1495 (2001).

26. Prinz, G. A., “Magnetoelectronics” ***Science***, 282 (5394): 1660–1663 (1998).

27. Prinz, G. A., “Magnetoelectronics applications” ***J. Magn. Magn. Mater.***, 2 (1–3): 57–68 (1999).

28. Galanakis, I. and Dederichs P.H., “Half-metallicity and Slater-Pauling behavior in the ferro-magnetic Heusler alloys”, ***Lect. Notes Phys.***, 676: 1–39 (2005).

29. Özdoğan, K., Şaşıoğlu, E. and Galanakis, I., “Fundamentals of half-metallic full-Heusler alloys”, spintronics: materials, applications, and devices, Lombardi, G. C. and Bianchi, G. E., ***Nova Science Pub Inc***, New York, 214 (2009).

30. Kilian, K. A. and Victora, R. H., “Electronic structure of $\mathrm{Ni_2MnIn}$ for use in spin injection”, ***J. Appl. Phys.***, 87 (9): 7064–7066 (2000).

31. Tanaka, C. T., Nowak, J. and Moodera, J. S., “Spin-polarized tunneling in a half-metallic ferromagnet”, ***J. Appl. Phys.***, 86 (11): 6239–6242 (1999).

32. Caballero, J. A., Park, Y. D., Childress, J. R., Bass, J., Chiang, W.-C., Reilly, A. C., Pratt, W. P. and Petroff, F., "Magnetoresistance of NiMnSb-based multilayers and spin valves" ***J. Vac. Sci. Technol. A***, 16 (3): 1801–1805 (1998).

33. Galanakis, I., Mavropoulos, P. and Dederichs, P. H., "Electronic structure and Slater-Pauling behaviour in half-metallic Heusler alloys calculated from first principles" ***J. Phys. D:Appl. Phys.***, 39 (5): 765–775 (2006).

34. Kübler, J., "First principle theory of metallic magnetism", ***Physica B+C***, 127 (1–3): 257–263 (1984).

35. Irkhin, V. Y. and Katsnelson, M. I., "Half- metallic ferromagnets", ***Phys. Usp.***, 37 (7): 659–676 (1994).

36. Dieny B., Speriosu, V.S., Parkin, S. S. P., Gurney, B. A., Wilhoit, D. R. and Mauri, D., "Giant magnetoresistive in soft ferromagnetic multilayers", ***Phys. Rev. B***, 43 (1): 1297–1300 (1991).

37. Schmidt, G., Ferrand, D., Molenkamp, L. W., Filip, A., T. and Van Wees, B. J., "Fundamental obstacle for electrical spin injection from a ferromagnetic metal into a diffusive semiconductor", ***Phys. Rev. B***, 62 (8): R4790–R4793 (2000).

38. Fiederling, R., Keim, M., Reuscher, G., Ossau, W., Schmidt, G., Waag, A. and Molenkamp, L.W., "Injection and detection of a spin-polarized current in a light-emitting diode", ***Nature***, 402 (6763): 787–790 (1999).

39. Ohno, Y., Young, D. K., Beschhoten, B., Matsukura, F., Ohno, H. and Awschalom, D. D., "Electrical spin injection in a ferromagnetic semiconductor heterostructure", ***Nature***, 402 (6763): 790–792 (1999).

40. Miura, Y., Shirai, M. and Nagao, K., "Ab initio study on stability of half-metallic Co-based full-Heusler alloys", ***J. Appl. Phys.***, 99 (8): 08J112 (2006).

41. Kandpal, H. C., Fecher, G. H., Felser, C. and Schönhense, G., "Correlation in the transition-metal-based Heusler compounds $\mathrm{Co_2MnSi}$ and $\mathrm{Co_2FeSi}$" ***Phys. Rev. B***, 73 (9): 094422 (2006).

42. Shirai, M., "Possible half-metallic ferromagnetism in zinc blende CrSb and CrAs" ***J. Appl. Phys***, 93 (10): 6844–6846 (2003).

43. Picozzi, S., Continenza, A. and Freeman, A. J., "$\mathrm{Co_2MnX}$ $(\mathrm{X = Si,\ Ge,\ Sn})$ Heusler compounds: an ab initio study of their structural, electronic, and magnetic properties at zero and elevated pressure", ***Phys. Rev. B***, 66 (9): 094421 (2002).

44. Ishida, S., Fujii, S., Kashiwagi, S. and Asano, S., "Search for half-metallic compounds in $\mathrm{Co_2MnZ}$ ($\mathrm{Z =}$ IIIb, IVb, Vb element)" ***J. Phys. Soc. Japan***, 64 (6): 2152–2157 (1995).

45. Galanakis, I., Dederichs, P. H. and Papanikolaou, N., "Slater-Pauling behavior and origin of the half-metallicity of the full-Heusler alloys", ***Phys. Rev. B***, 66 (17): 174429 (2002).

46. Galanakis, I., Dederichs, P. H. and Papanikolaou, N., "Origin and properties of the gap in the half-ferromagnetic Heusler alloys", ***Phys. Rev. B***, 66 (13): 134428 (2002).

47. Galanakis, I. and Mavropoulos, Ph., "Spin-polarization and electronic properties of half-metallic Heusler alloys calculated from first principles", ***J. Phys.: Condens. Matter***, 19 (31): 315213 (2007).

48. Brown, P. J., Neumann, K. U., Webster, P. J. and Ziebeck, K. R. A., "The magnetization distributions in some Heusler alloys proposed as half-metallic ferromagnets", ***J. Phys.: Condens. Matter***, 12 (8): 1827–1835 (2000).

49. Kandpal, H. C., Fecher, G. H. and Felser, C., "Calculated electronic and magnetic properties of the half-metallic, transition metal based Heusler compounds", ***J. Phys. D: Appl. Phys.***, 40 (6): 1507–1523 (2007).

50. Block, T., Felser, C., Jakob, G., Ensling, J., Muhling, B., Gutlich, P., Beaumont, V., Studer, F. and Cava, R.J., "Large negative magnetoresistance effects in $\mathrm{Co_2Cr_{0.6}Fe_{0.4}Al}$", ***J. Solid State Chem.***, 176 (2): 646-651 (2003).

51. Wang, W. H., Przybylski, M., Kuch, W., Chelaru, L. I., Wang, J., Lu, Y. F., Barthel, J. and Kirschner, J., "Spin polarization of single-crystalline $\mathrm{Co_2MnSi}$ films grown by PLD on $\mathrm{GaAs}(0\,0\,1)$", ***J. Magn. Magn. Mater.***, 286 (SI): 336–339 (2005).

52. Wang, W. H., Przybylski, M., Kuch, W., Chelaru, L. I., Wang, J., Lu, Y. F., Barthel, J., Meyerheim, H. L. and Kirschner, J., "Magnetic properties and spin polarization of $\mathrm{Co_2MnSi}$ Heusler alloy thin films epitaxially grown on $\mathrm{GaAs}(001)$", ***Phys. Rev. B***, 71 (14): 144416 (2005).

53. Kammerer, S., Heitmann, S., Meyners, D., Sudfeld, D., Thomas, A., Htten, A. and Reiss, G., "Room-temperature preparation and magnetic behavior of $\mathrm{Co_2MnSi}$ thin films", ***J. Appl. Phys.***, 93 (10): 7945–7947 (2003).

54. Inomata, K., Okamura and Tezuka, N., "Tunnel magnetoresistance using full-Heusler alloys", ***J. Magn. Magn. Mater.***, 282 (SI): 269–274 (2004).

55. Kammerer, S., Thomas, A., Htten, A. and Reiss, G., "$\mathrm{Co_2MnSi}$ Heusler alloy as magnetic electrodes in magnetic tunnel junctions" ***Appl. Phys. Lett.***, 85 (1): 79–81 (2004).

56. Şaşıoğlu, E., Sandratskii, L. M., Bruno, P. and Galanakis, I., "Exchange interactions and temperature dependence of magnetization in half-metallic Heusler alloys", ***Phys. Rev. B***, 72 (18): 184415 (2005).

57. Hamzic\', A., Asomoza, R. and Campbell, I. A., "The transport properties of Heusler alloys: ideal local moment ferromagnets", ***J. Phys. F: Met. Phys.***, 11 (7): 1441–1447 (1981).

58. Kübler, J., Williams, A. R. and Sommers, C. B., "Formation and coupling of magnetic moments in Heusler alloys", ***Phys. Rev. B***, 28 (4): 1745–1755 (1983).

59. Slater, J. C., “The Ferromagnetism of nickel. II. temperature effects”, ***Phys. Rev.*** 49 (12): 931–937 (1936).

60. Pauling, L., “The nature of the interatomic forces in metals”, ***Phys. Rev.***, 54 (11): 899-904 (1938).

61. Kübler, J., “Theory of itinerant electron magnetism”, ***Oxford University Press***, Oxford, New York, 396 (2000).

62. QUANTUM-ESPRESSO is a community project for high-quality quantum-simulation software, based on density-functional theory, and coordinated by Paolo Gianozzi. See <http://www.quantum-espresso.org and http://www.pwscf.org>

63. Giannozzi, P., Baroni, S., Bonini, N., Calandra, M., Car, R., Cavazzoni, C., Ceresoli, D., Chiarotti, G. L., Cococcioni, M., Dabo, I., Corso, A. D., de Gironcoli, S., Fabris, S., Fratesi, G., Gebauer, R., Gerstmann, U., Gougoussis, C., Kokalj, A., Lazzeri, M., Martin-Samos, L., Marzari, N., Mauri, F., Mazzarello, R., Paolini, S., Pasquarello, A., Paulatto, L., Sbraccia, C., Scandolo, S., Sclauzero, G., Seitsonen, A.P., Smogunov, A., Umari, P. and Wentzcovitch, R. M., “QUANTUM ESPRESSO: a modular and open-source software project for quantum simulations of materials”, ***J. Phys.: Condens. Matter***, 21 (39): 395502 (2009).

64. Monkhorst, H. J. and Pack, J. D., “Special points for Brillouin-zone integrations”, ***Phys. Rev. B***, 13 (12): 5188–5192 (1976).

65. Methfessel, M. and Paxton, A. T., “High-precision sampling for Brillouin-zone integration in metals”, ***Phys. Rev. B***, 40 (6): 3616–3621 (1989).

66. Ernest R. D., “The iterative calculation of a few of the lowest eigenvalues and corresponding eigenvectors of large real-symmetric matrices”, ***Journal of Computational Physics***, 17 (1): 87–94 (1975).

67. Vinet, P., Ferrante, J., Smith, J. R. and Rose, J. S., “A universal equation of state for solids”, ***J. Phys. C***, 19 (20): L467–L473 (1986).

68. Cohen, R. E., Gülseren O and Hamley R. J., “Accuracy of equation of state formulations”, ***Am. Mineral***, 85: 338–344 (2000).

69. Gökoğlu, G. and Gülseren, O., “Electronic structure of half-metallic ferromagnet $\mathrm{Co_2MnSi}$ at high-pressure”, ***Eur. Phys. J. B***, 76 (2): 321–326 (2010).

70. Hao, A, Yang, X., Wang, X., Zhu, Y., Liu, X. and Liu, R., “First-principles investigations on electronic, elastic and optical properties of XC ($\mathrm{X} = \mathrm{Si}, \mathrm{Ge}$, and Sn) under high pressure”, ***J. Appl. Phys.***, 108 (6): 063531 (2010).

AUTOBIOGRAPHY

Ulvi KANBUR was born in Rize in 1986. After graduating from Rize Fener Super High School in 2004 he started to study physics in Dokuz Eylül University from which he graduated in 2009. He is now working at Karabük University as a research assistant on physics. He has completed his M. Sc. degree on 2011 with a thesis on "First Principles Investigation of Electronic and Magnetic Properties of the Half-Metallic Heusler Alloys".

Publications

1) Kanbur, U., GÖKOĞLU, G., "Half-metallic magnetism of $\mathrm{Co2CrX}\,(\mathrm{X} = \mathrm{As},\ \mathrm{Sb})$ Heusler compounds: An ab initio study", ***Journal of Magnetism and Magnetic Materials***, 323 (9): 1156–1160 (2011).